# Supplementary Information (SI)

# Discovery of a new binding site for the possible gain in neomorphic activity in R132H_IDH1

**Nandeshwar,[1,†] Abhipsa Sekhar Biswal,[2,†] Soumit Chatterjee,[2,*] and Umakanta Tripathy[1,*]**

[1]Department of Physics, Indian Institute of Technology (Indian School of Mines) Dhanbad, Dhanbad, 826004, Jharkhand, India.

[2]Department of Chemistry and Chemical Biology, Indian Institute of Technology (Indian School of Mines) Dhanbad, Dhanbad, 826004, Jharkhand, India.

[1*]**Corresponding author E-mail**: utripathy@iitism.ac.in

[2*]**Corresponding author E-mail**: soumit@iitism.ac.in

[†] **Equal contribution**

**Video 1**: ICT_NADPH-bound R132H_IDH1 indicates a new binding site.

Video
1_IDH1_JCIM_IITISM.r

**Table S1.** Root mean square deviation (RMSD) of R132H_IDH1 and WT_IDH1 at various pH values (7.6, 7.4, 7.2, 6.8, and 5.6).

| System Description | RMSD (mean ± std. deviation) (nm) |
|---|---|
| WT_IDH1_7.6 | 0.34 ± 0.03 |
| R132H_IDH1_7.6 | 0.53 ± 0.07 |
| WT_IDH1_7.4 | 0.35 ± 0.04 |
| R132H_IDH1_7.4 | 0.36 ± 0.03 |
| WT_IDH1_7.2 | 0.46 ± 0.06 |
| R132H_IDH1_7.2 | 0.58 ± 0.09 |
| WT_IDH1_6.8 | 0.35 ± 0.03 |
| R132H_IDH1_6.8 | 0.60 ± 0.08 |
| WT_IDH1_5.6 | 0.28 ± 0.02 |
| R132H_IDH1_5.6 | 0.44 ± 0.03 |

**Table S2.** Radius of Gyration (Rg) of R132H_IDH1 and WT_IDH1 at various pH values (7.6, 7.4, 7.2, 6.8, and 5.6).

| System Description | Rg (mean ± std. deviation) (nm) |
|---|---|
| WT_IDH1_7.6 | 2.30 ± 0.02 |
| R132H_IDH1_7.6 | 2.25 ± 0.03 |
| WT_IDH1_7.4 | 2.31 ± 0.02 |
| R132H_IDH1_7.4 | 2.31 ± 0.02 |
| WT_IDH1_7.2 | 2.27 ± 0.03 |
| R132H_IDH1_7.2 | 2.29 ± 0.04 |
| WT_IDH1_6.8 | 2.30 ± 0.01 |
| R132H_IDH1_6.8 | 2.29 ± 0.03 |
| WT_IDH1_5.6 | 2.30 ± 0.01 |
| R132H_IDH1_5.6 | 2.32 ± 0.01 |

**Table S3.** Solvent accessible surface area (SASA) hydrophilic of R132H_IDH1 and WT_IDH1 at various pH values (7.6, 7.4, 7.2, 6.8, and 5.6).

| System Description | SASA Hydrophilic (mean ± std. deviation) ($nm^2$) |
|---|---|
| WT_IDH1_7.6 | 269.04 ± 3.28 |
| R132H_IDH1_7.6 | 273.61 ± 3.94 |
| WT_IDH1_7.4 | 274.79 ± 4.26 |
| R132H_IDH1_7.4 | 276.17 ± 3.48 |
| WT_IDH1_7.2 | 269.63 ± 3.90 |
| R132H_IDH1_7.2 | 273.73 ± 4.02 |
| WT_IDH1_6.8 | 265.12 ± 4.29 |
| R132H_IDH1_6.8 | 269.67 ± 3.60 |
| WT_IDH1_5.6 | 267.61 ± 3.21 |
| R132H_IDH1_5.6 | 268.70 ± 4.05 |

**Table S4.** Solvent accessible surface area (SASA) hydrophobic of R132H_IDH1 and WT_IDH1 at various pH values (7.6, 7.4, 7.2, 6.8, and 5.6).

| System Description | SASA Hydrophobic (mean ± std. deviation) ($nm^2$) |
|---|---|
| WT_IDH1_7.6 | 180.80 ± 2.66 |
| R132H_IDH1_7.6 | 186.12 ± 3.01 |
| WT_IDH1_7.4 | 186.21 ± 3.45 |
| R132H_IDH1_7.4 | 184.77 ± 3.82 |
| WT_IDH1_7.2 | 192.23 ± 3.31 |
| R132H_IDH1_7.2 | 186.75 ± 2.75 |
| WT_IDH1_6.8 | 182.69 ± 3.24 |
| R132H_IDH1_6.8 | 183.94 ± 2.87 |
| WT_IDH1_5.6 | 183.63 ± 2.31 |
| R132H_IDH1_5.6 | 189.75 ± 2.55 |

**Table S5.** Comparative analysis of domain flexibility between WT_IDH1 and R132H_IDH1 at pH 7.6.

| Domain | Residue Range (WT) | Avg. RMSF (WT) (nm) | SD (WT) (nm) | Residue Range (R132H) | Avg. RMSF (R132H) (nm) | SD (R132H) (nm) | Interpretation |
|---|---|---|---|---|---|---|---|
| 1 | 46–55 | 0.214 | 0.028 | 46–55 | 0.246 | 0.027 | Slightly increased flexibility in mutant |
| 2 | 79–98 | 0.223 | 0.034 | 77–95 | 0.523 | 0.201 | Strong increase in flexibility in mutant |
| 3 | 116–120 | 0.205 | 0.0264 | - | - | - | Not present in mutant |
| 4 | 136–184 | 0.344 | 0.104 | 141–183 | 0.464 | 0.155 | Markedly increased flexibility in mutant |
| 5 | - | - | - | 213–219 | 0.297 | 0.067 | A new flexible domain pops up in mutant |
| 6 | 321–323 | 0.223 | 0.011 | 310–325 | 0.214 | 0.028 | Slightly reduced average flexibility, but the domain of mutant is extended to 15 residues whereas it remains on 3 in case of wild-type |
| 7 | 379–384 | 0.207 | 0.016 | 382–385 | 0.215 | 0.015 | Nearly identical flexibility |

**Table S6.** Comparative analysis of domain flexibility between WT IDH1 and R132H IDH1 at pH 7.4.

| Domain | Residue Range (WT) | Avg. RMSF (WT) (nm) | SD (WT) (nm) | Residue Range (R132H) | Avg. RMSF (R132H) (nm) | SD (R132H) (nm) | Interpretation |
|---|---|---|---|---|---|---|---|
| 1 | 45–55 | 0.241 | 0.024 | 46–54 | 0.202 | 0.015 | Decreased flexibility in mutant |
| 2 | 76–99 | 0.530 | 0.197 | 76–93 | 0.477 | 0.149 | Slight decrease in flexibility in mutant |
| 3 | 116–123 | 0.242 | 0.058 | 116–123 | 0.284 | 0.037 | Slight increase in flexibility in mutant |
| 4 | 138–180 | 0.271 | 0.052 | 134–180 | 0.383 | 0.135 | Marked increase in flexibility in mutant |
| 5 | 213–216 | 0.214 | 0.021 | - | - | - | Not present in mutant |
| 6 | 310–314 | 0.216 | 0.044 | 310–314 | 0.300 | 0.062 | Increased flexibility in mutant |
| 7 | 320–324 | 0.215 | 0.016 | - | - | - | Not represented in mutant |
| 8 | 378–389 | 0.268 | 0.043 | 378–389 | 0.256 | 0.037 | Slight decrease in flexibility in mutant |

**Table S7.** Comparative analysis of domain flexibility between WT IDH1 and R132H IDH1 at pH 7.2.

| Domain | Residue Range (WT) | Avg. RMSF (WT) (nm) | SD (WT) (nm) | Residue Range (R132H) | Avg. RMSF (R132H) (nm) | SD (R132H) (nm) | Interpretation |
|---|---|---|---|---|---|---|---|
| 1 | 44–57 | 0.302 | 0.074 | 47–55 | 0.204 | 0.014 | Decreased flexibility in mutant |
| 2 | 78–98 | 0.312 | 0.094 | 76–93 | 0.411 | 0.123 | Increased flexibility in mutant |
| 3 | 116–123 | 0.321 | 0.042 | - | - | - | Not represented in mutant |
| 4 | 135–185 | 0.653 | 0.240 | 135–184 | 0.671 | 0.295 | Comparable but slightly more variable in mutant |
| 5 | 211–220 | 0.296 | 0.093 | 212–222 | 0.241 | 0.034 | Decreased flexibility in mutant |
| 6 | 320–323 | 0.221 | 0.010 | 314–325 | 0.234 | 0.033 | Slight increase in mutant with higher variability |
| 7 | 380–389 | 0.237 | 0.029 | 380–385 | 0.225 | 0.015 | Slightly reduced flexibility in mutant |
| 8 | - | - | - | 285–286 | 0.224 | 0.010 | Additional flexible region present only in mutant |

**Table S8.** Comparative analysis of domain flexibility between WT IDH1 and R132H IDH1 at pH 6.8.

| Domain | Residue Range (WT) | Avg. RMSF (WT) (nm) | SD (WT) (nm) | Residue Range (R132H) | Avg. RMSF (R132H) (nm) | SD (R132H) (nm) | Interpretation |
|---|---|---|---|---|---|---|---|
| **1** | – | – | – | 46–55 | 0.23461 | 0.02209 | Additional stable region present only in mutant |
| **2** | 79–91 | 0.24443 | 0.02549 | 79–93 | 0.30887 | 0.04821 | Increased flexibility in mutant |
| **3** | 136–185 | 0.31188 | 0.11177 | 136–182 | 0.51079 | 0.19193 | Significantly increased flexibility in mutant |
| **4** | 212–221 | 0.24628 | 0.03838 | 213–217 | 0.22972 | 0.03837 | Slightly decreased flexibility in mutant |
| **5** | – | – | – | 382–385 | 0.22055 | 0.01337 | Additional stable region present only in mutant |

**Table S9.** Comparative analysis of domain flexibility between WT IDH1 and R132H IDH1 at pH 5.6.

| Comparative Analysis of Domain Flexibility Between WT IDH1 and R132H IDH1 (pH 5.6) | | | | | | | |
|---|---|---|---|---|---|---|---|
| **Domain** | **Residue Range (WT)** | **Avg. RMSF (WT) (nm)** | **SD (WT) (nm)** | **Residue Range (R132H)** | **Avg. RMSF (R132H) (nm)** | **SD (R132H) (nm)** | **Interpretation** |
| **1** | – | – | – | 46–54 | 0.216 | 0.022 | Additional flexible region present only in mutant |
| **2** | – | – | – | 79–94 | 0.401 | 0.093 | Additional highly flexible region present only in mutant |
| **3** | 119–122 | 0.230 | 0.020 | – | – | – | Not present in mutant |
| **4** | 145–178 | 0.200 | 0.052 | 135–182 | 0.410 | 0.110 | Significantly increased flexibility in mutant |
| **5** | 214–215 | 0.238 | 0.048 | 214–216 | 0.224 | 0.011 | Slightly reduced flexibility in mutant |
| **6** | 257–260 | 0.214 | 0.006 | – | – | – | Not present in mutant |
| **7** | 310–311 | 0.235 | 0.040 | 310–311 | 0.247 | 0.047 | Slight increase in mutant |
| **8** | 383–384 | 0.210 | 0.020 | – | – | – | Not present in mutant |

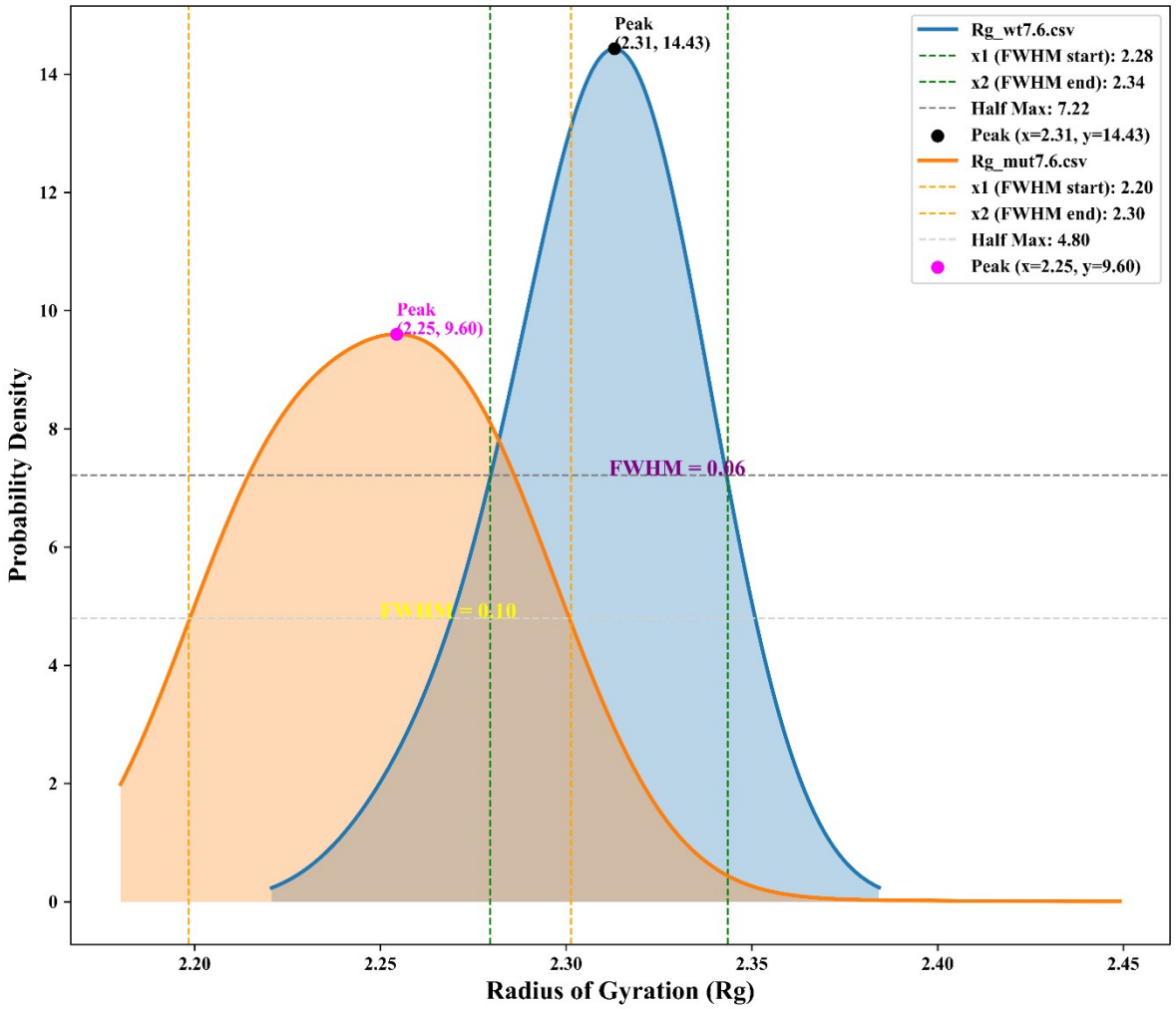


**Figure S1**. Probability density versus Radius of gyration plot of IDH1_R132H and WT_IDH1 for pH 7.6.

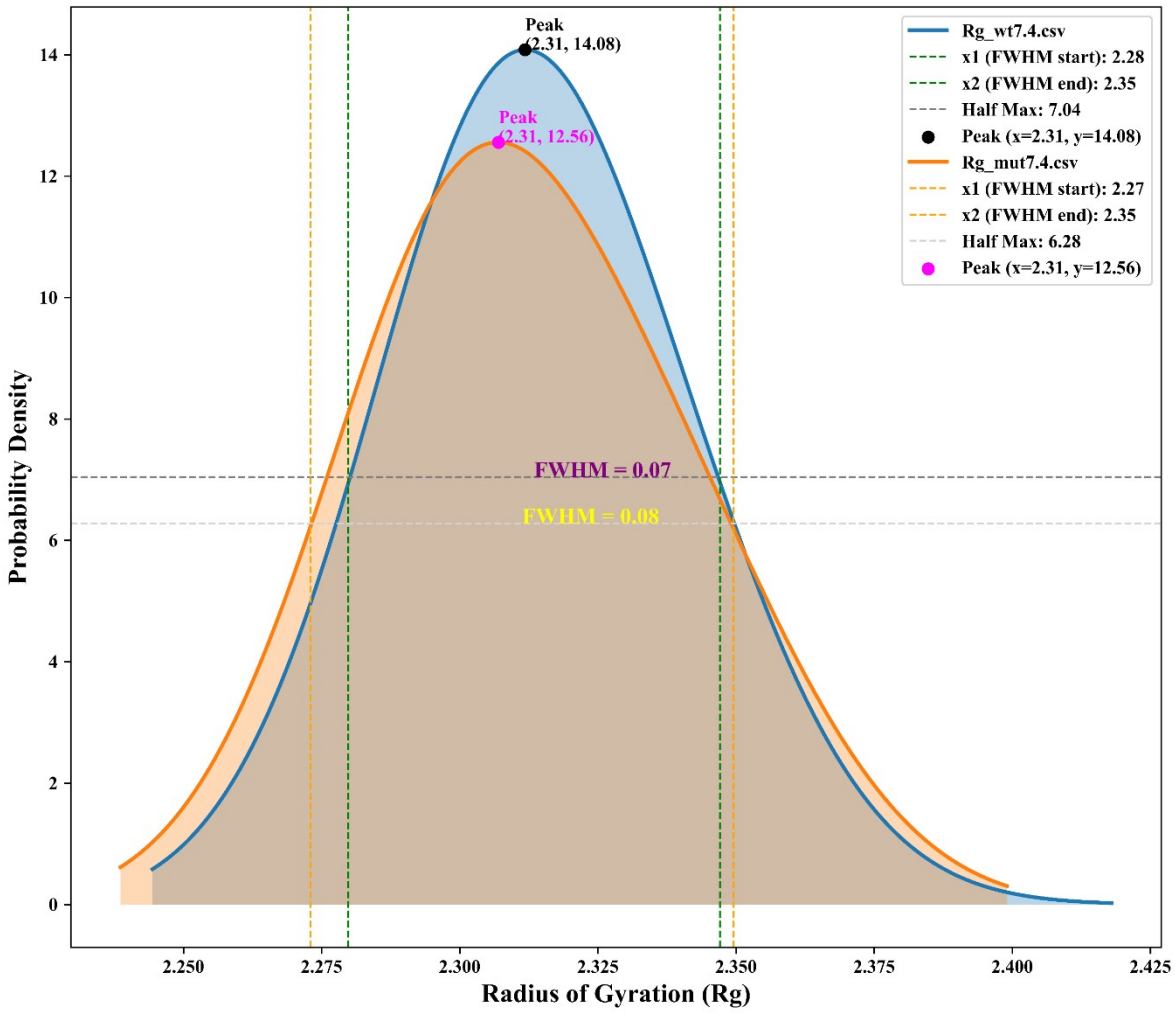


**Figure S2**. Probability density versus Radius of gyration plot of IDH1_R132H and WT_IDH1 for pH 7.4.

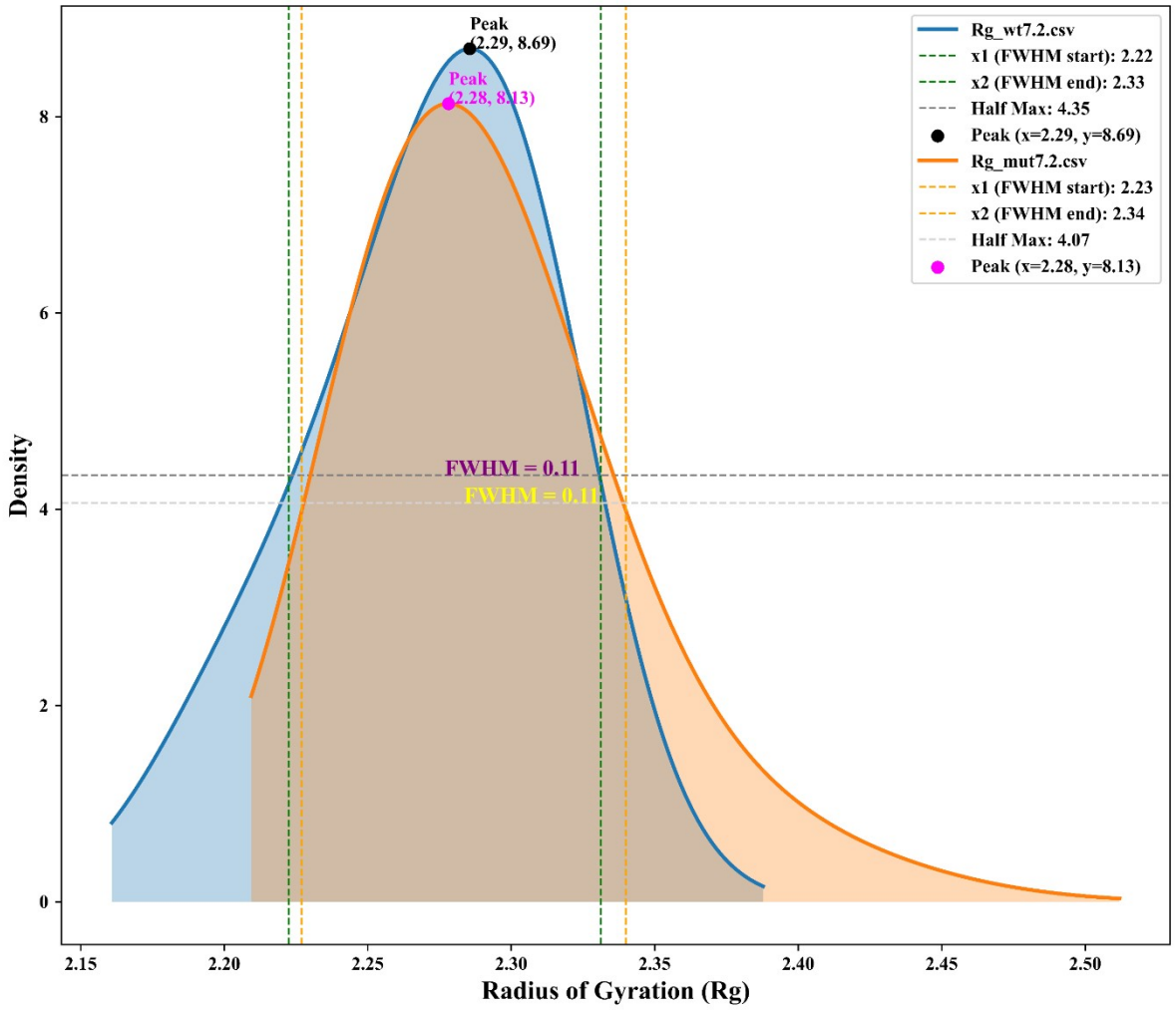


**Figure S3**. Probability density versus Radius of gyration plot of IDH1_R132H and WT_IDH1 for pH 7.2.

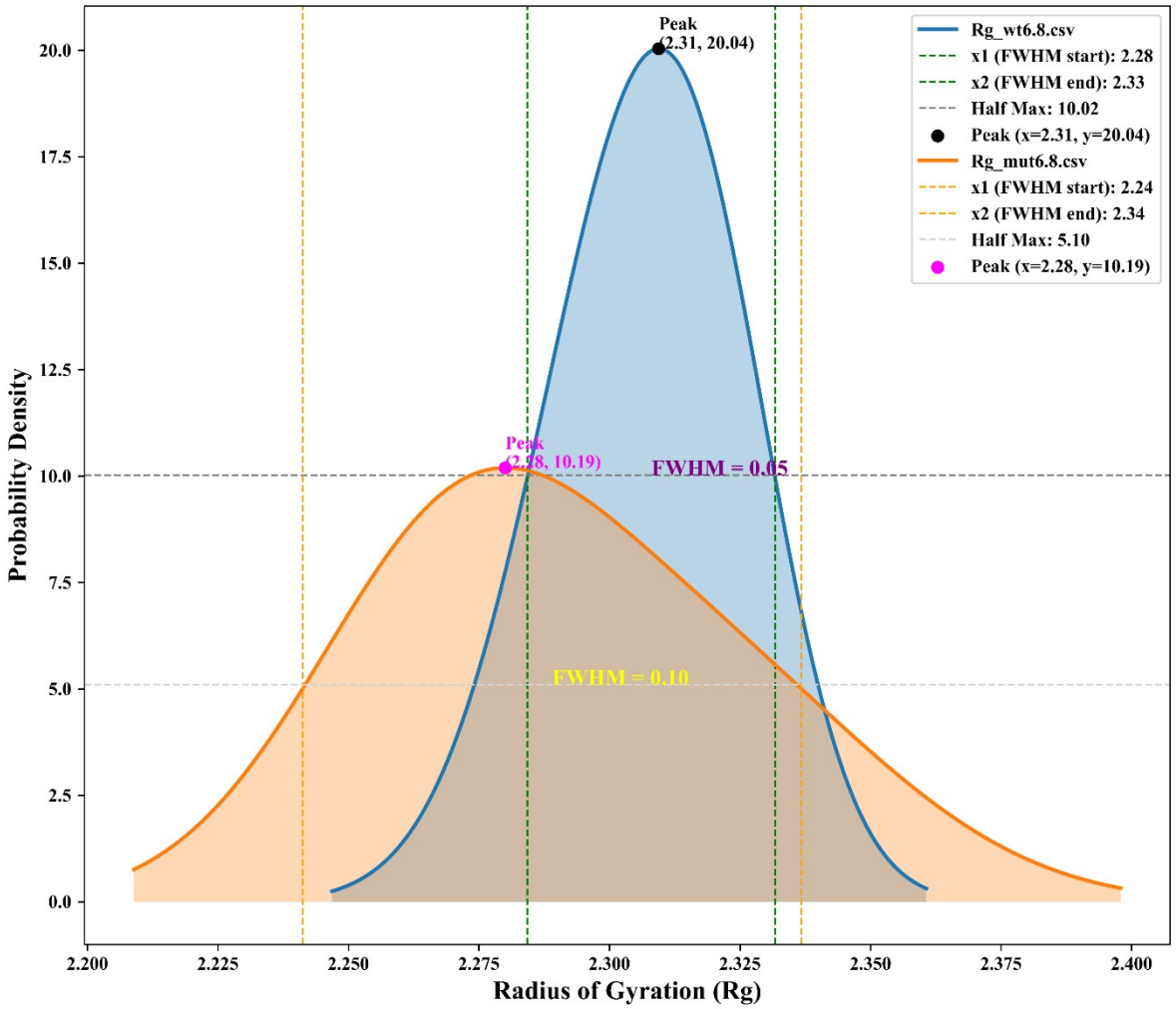


**Figure S4.** Probability density versus Radius of gyration plot of IDH1_R132H and WT_IDH1 for pH 6.8.

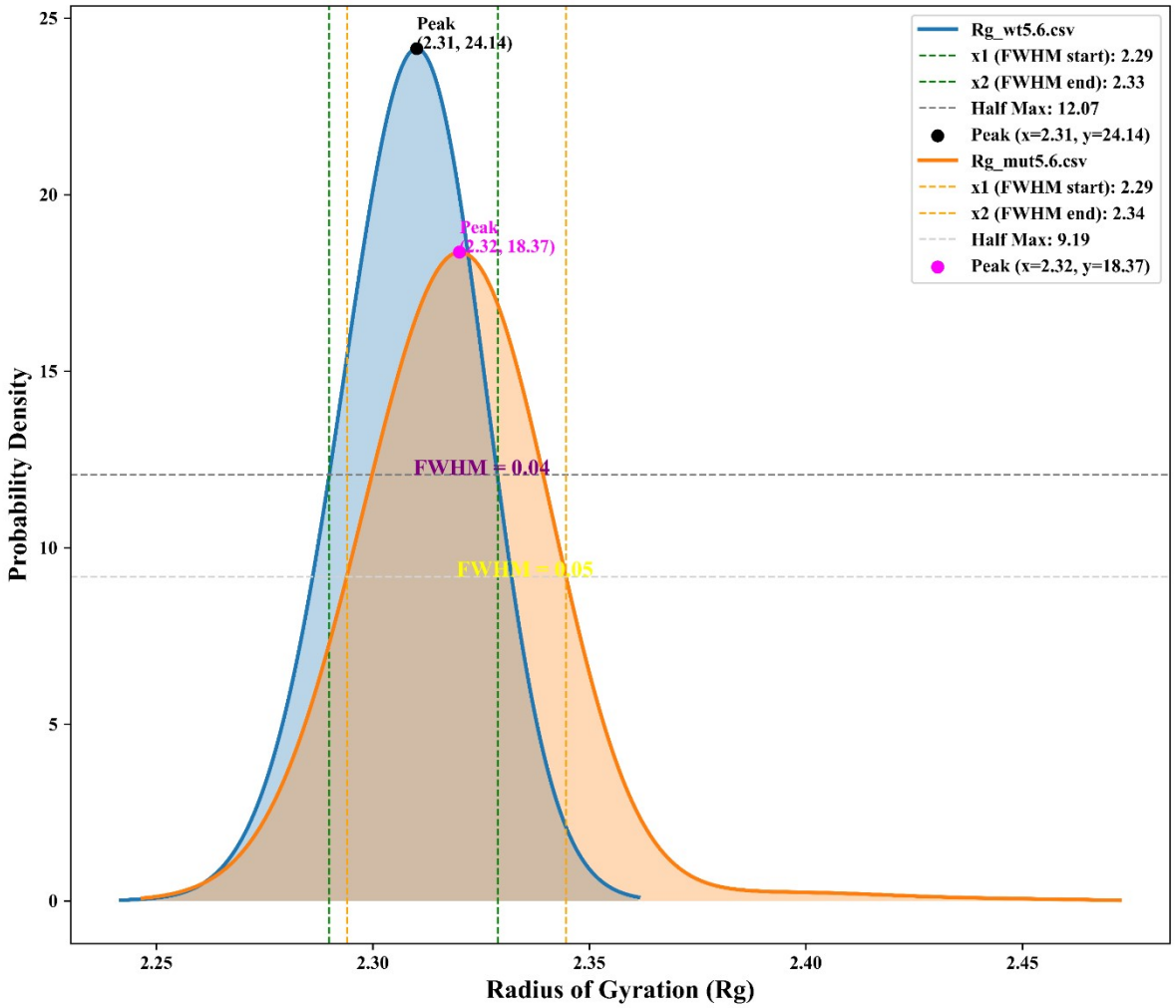


**Figure S5.** Probability density versus Radius of gyration plot of IDH1_R132H and WT_IDH1 for pH 5.6.

A

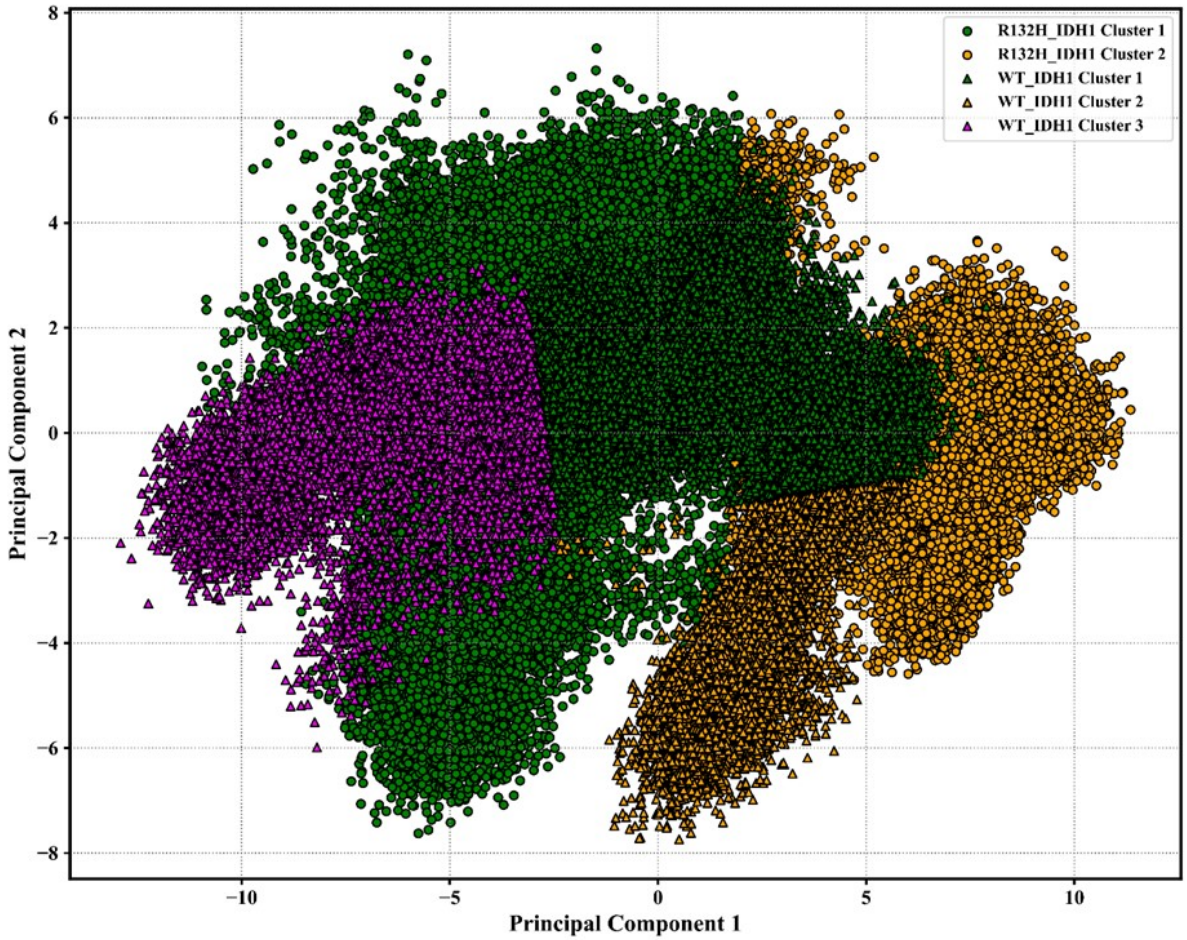
R132H_IDH1 Cluster 1
R132H_IDH1 Cluster 2
WT_IDH1 Cluster 1
WT_IDH1 Cluster 2
WT_IDH1 Cluster 3
Principal Component 2
Principal Component 1
8
6
4
2
0
−2
−4
−6
−8
−10
−5
0
5
10

B

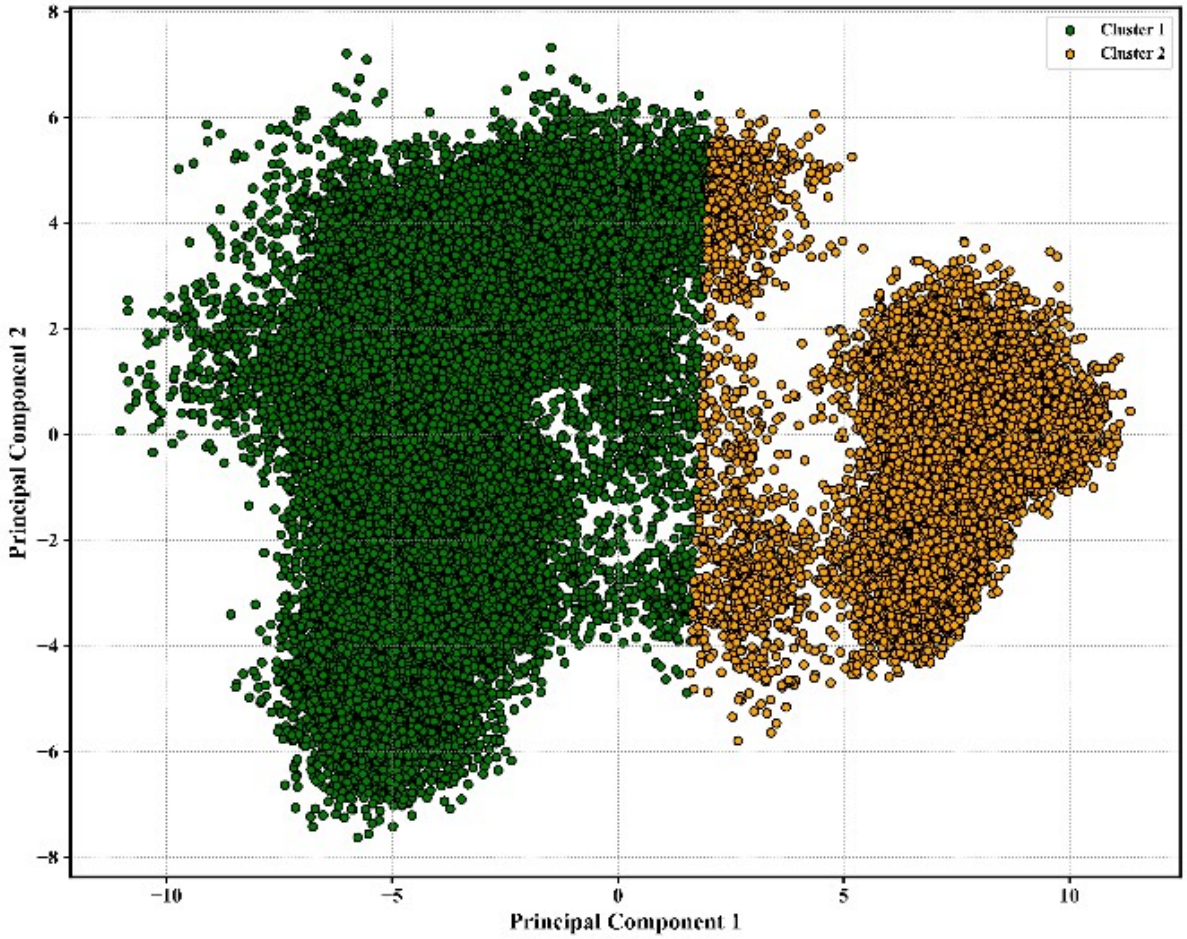
Cluster 1
Cluster 2
Principal Component 2
Principal Component 1
8
6
4
2
0
−2
−4
−6
−8
−10
−5
0
5
10

C

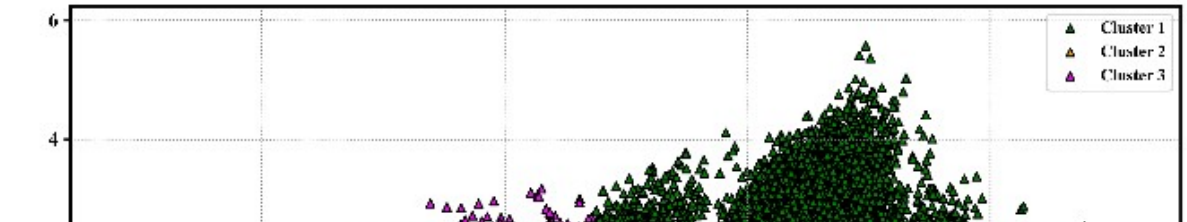
Cluster 1
Cluster 2
Cluster 3
6
4

D

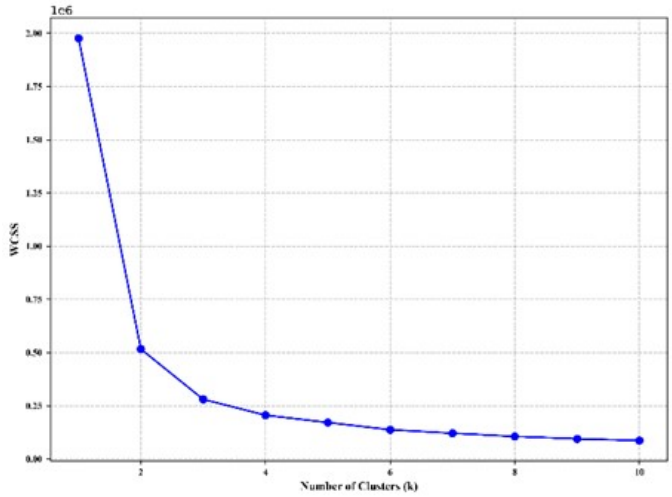


E

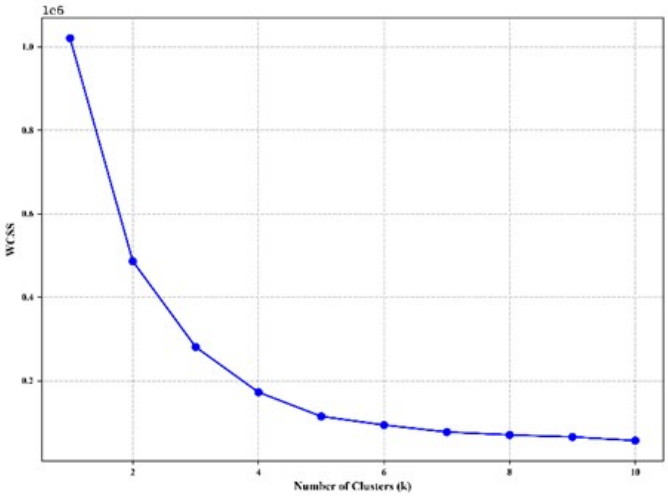


F

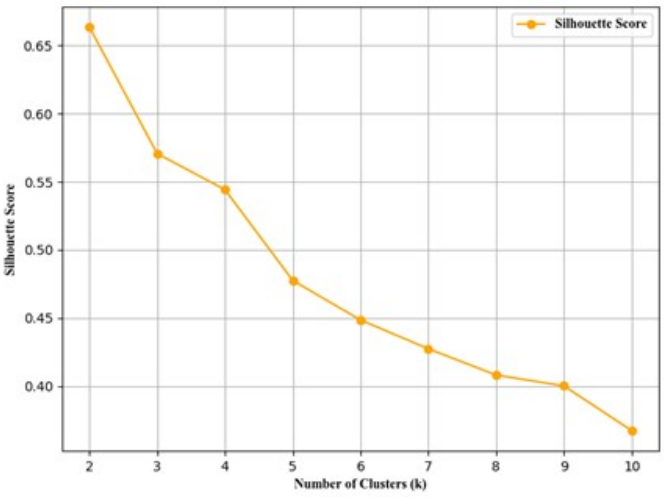


G

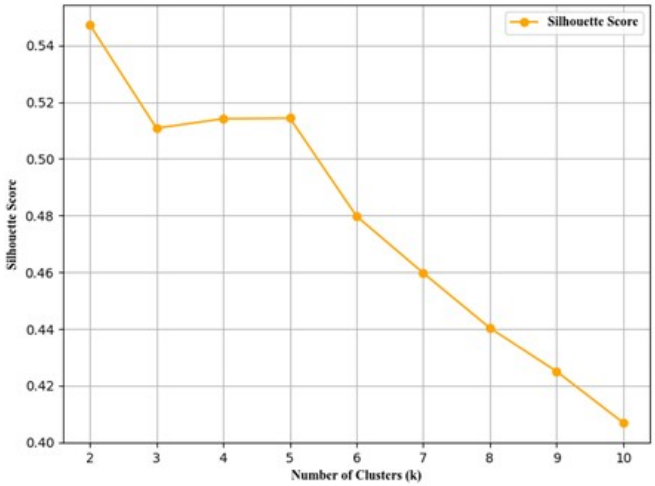


**Figure S6**. Cluster plot of PC1 vs PC2 for (A) comparing conformational space of R132H_IDH1 and WT_IDH1, (B) conformational space of R132H_IDH1, (C) conformational space of WT_IDH1, Elbow plot for (D) R132H_IDH1, (E) WT_IDH1, and Silhouette plot for (F) R132H_IDH1, (G) WT_IDH1 at pH 7.6.

A

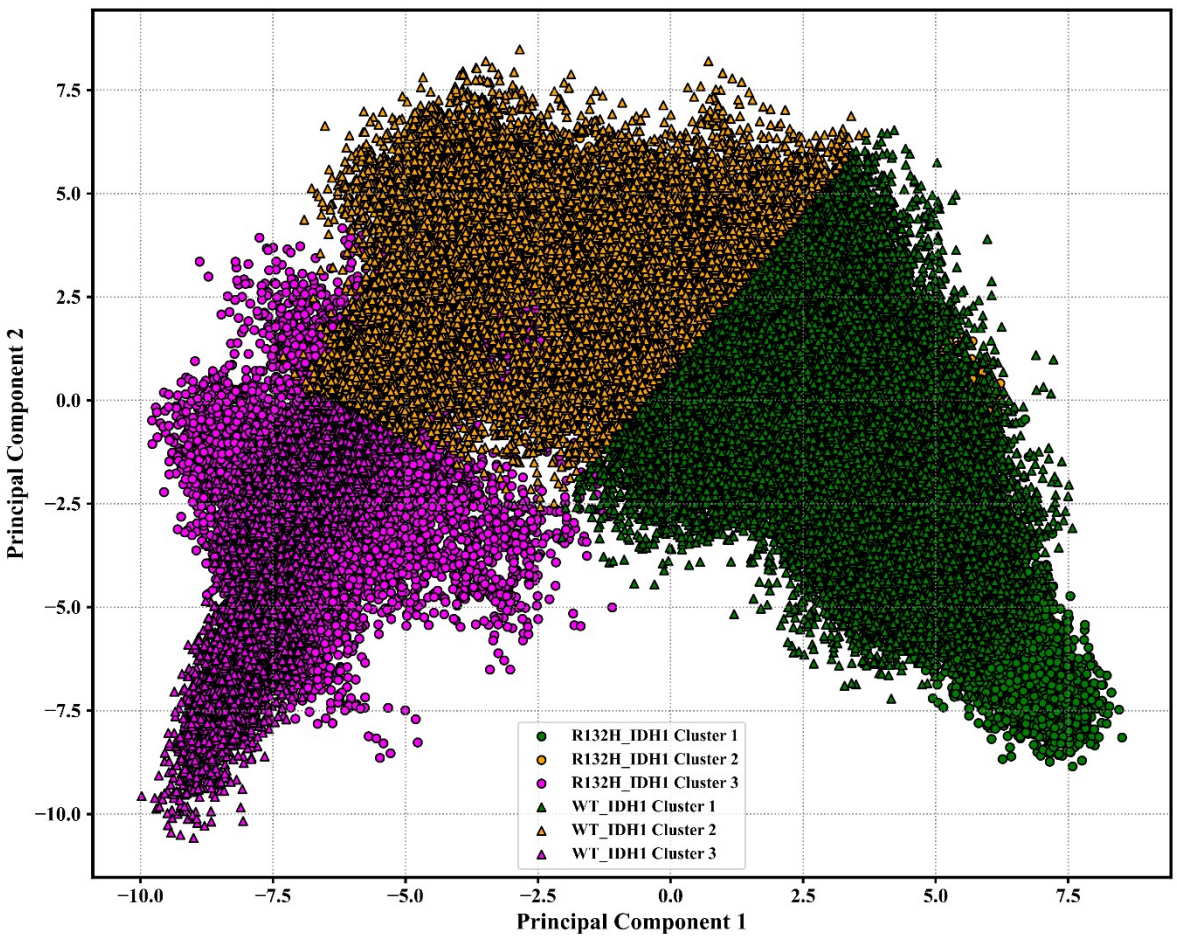
Principal Component 2
Principal Component 1
7.5
5.0
2.5
0.0
−2.5
−5.0
−7.5
−10.0
−10.0
−7.5
−5.0
−2.5
0.0
2.5
5.0
7.5
R132H_IDH1 Cluster 1
R132H_IDH1 Cluster 2
R132H_IDH1 Cluster 3
WT_IDH1 Cluster 1
WT_IDH1 Cluster 2
WT_IDH1 Cluster 3

B

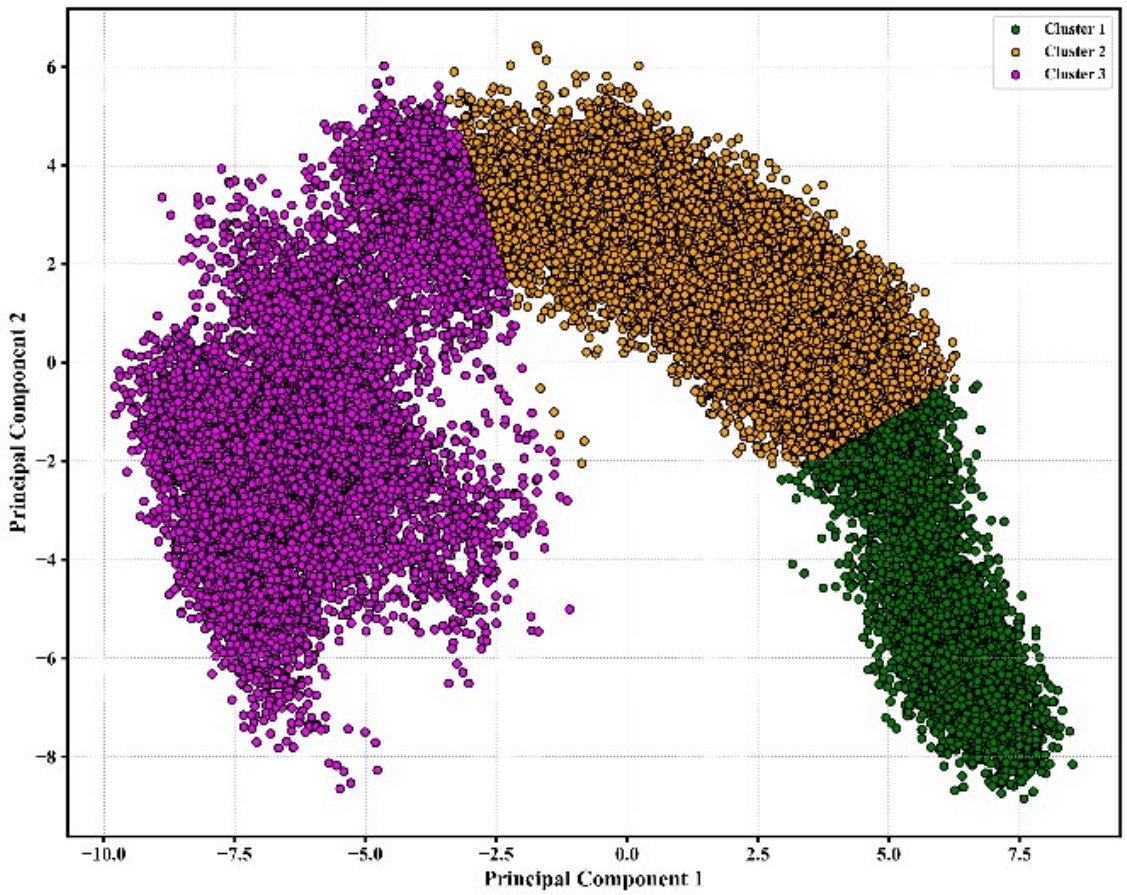
Cluster 1
Cluster 2
Cluster 3
Principal Component 2
Principal Component 1
6
4
2
0
−2
−4
−6
−8
−10.0
−7.5
−5.0
−2.5
0.0
2.5
5.0
7.5

C

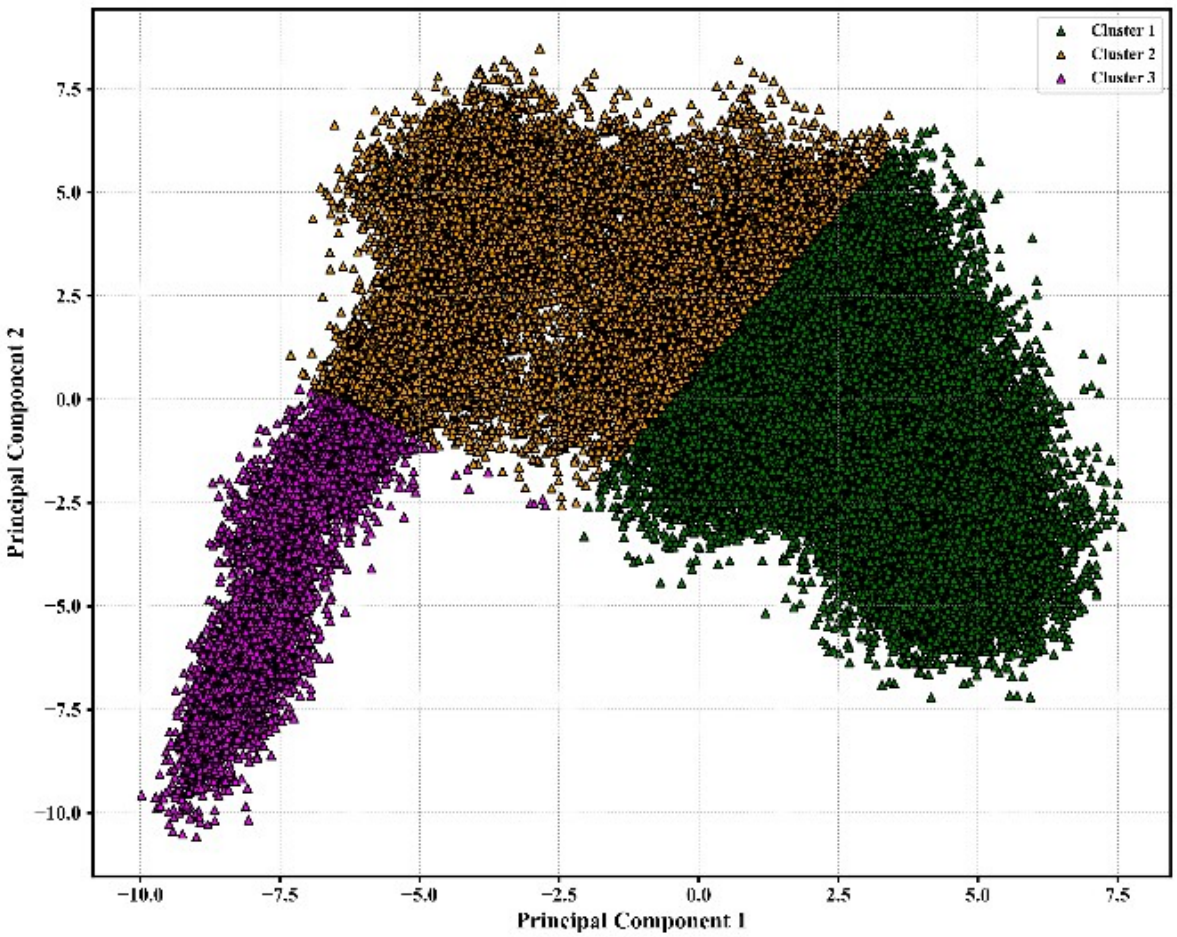
Cluster 1
Cluster 2
Cluster 3
Principal Component 2
Principal Component 1
7.5
5.0
2.5
0.0
−2.5
−5.0
−7.5
−10.0
−10.0
−7.5
−5.0
−2.5
0.0
2.5
5.0
7.5

D E

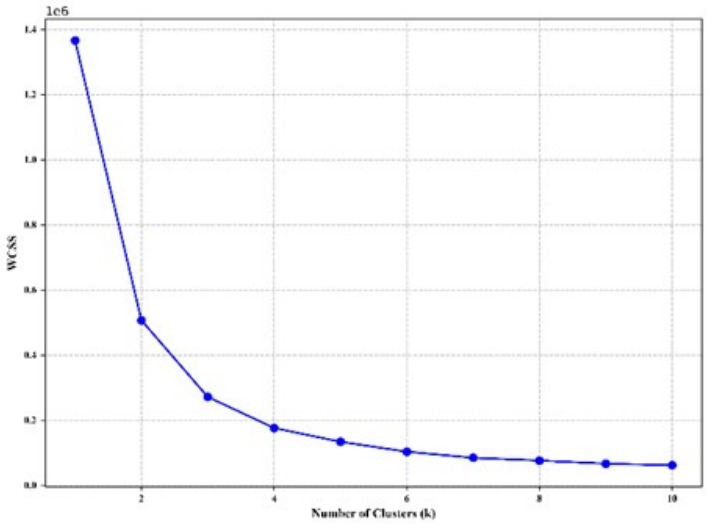


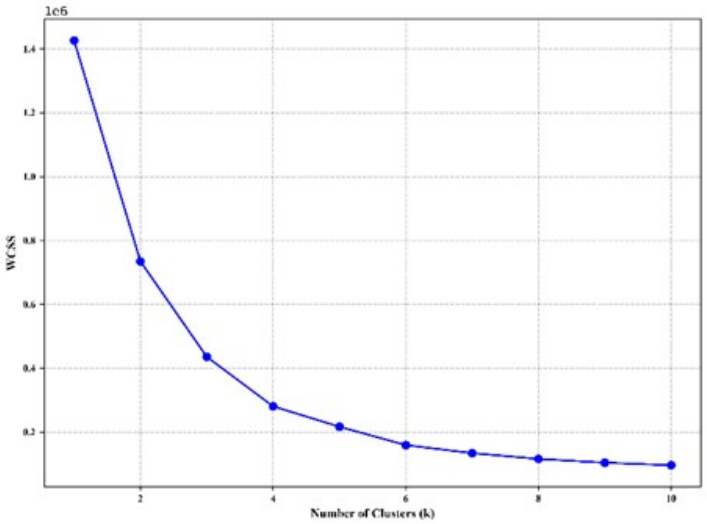


F

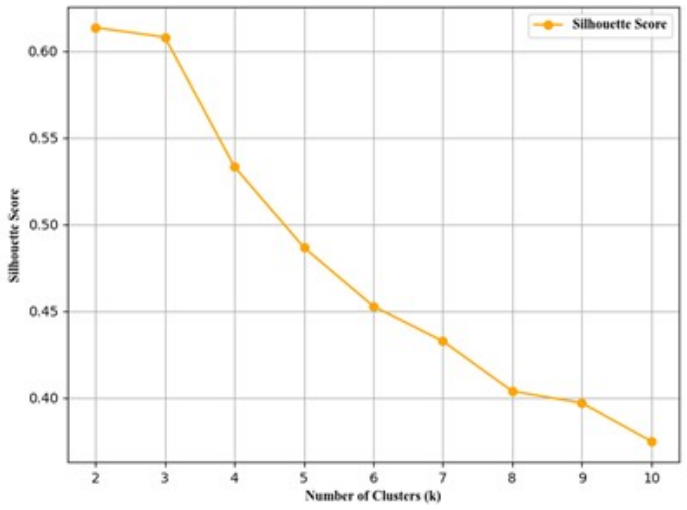


G

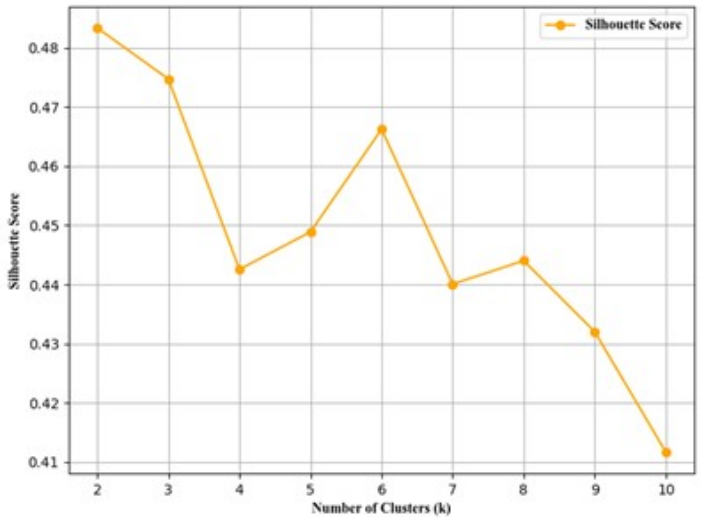


**Figure S7.** Cluster plot of PC1 vs PC2 for (A) comparing conformational space of R132H_IDH1 and WT_IDH1, (B) conformational space of R132H_IDH1, (C) conformational space of WT_IDH1, Elbow plot for (D) R132H_IDH1, (E) WT_IDH1, and Silhouette plot for (F) R132H_IDH1, (G) WT_IDH1 at pH 7.4.

A

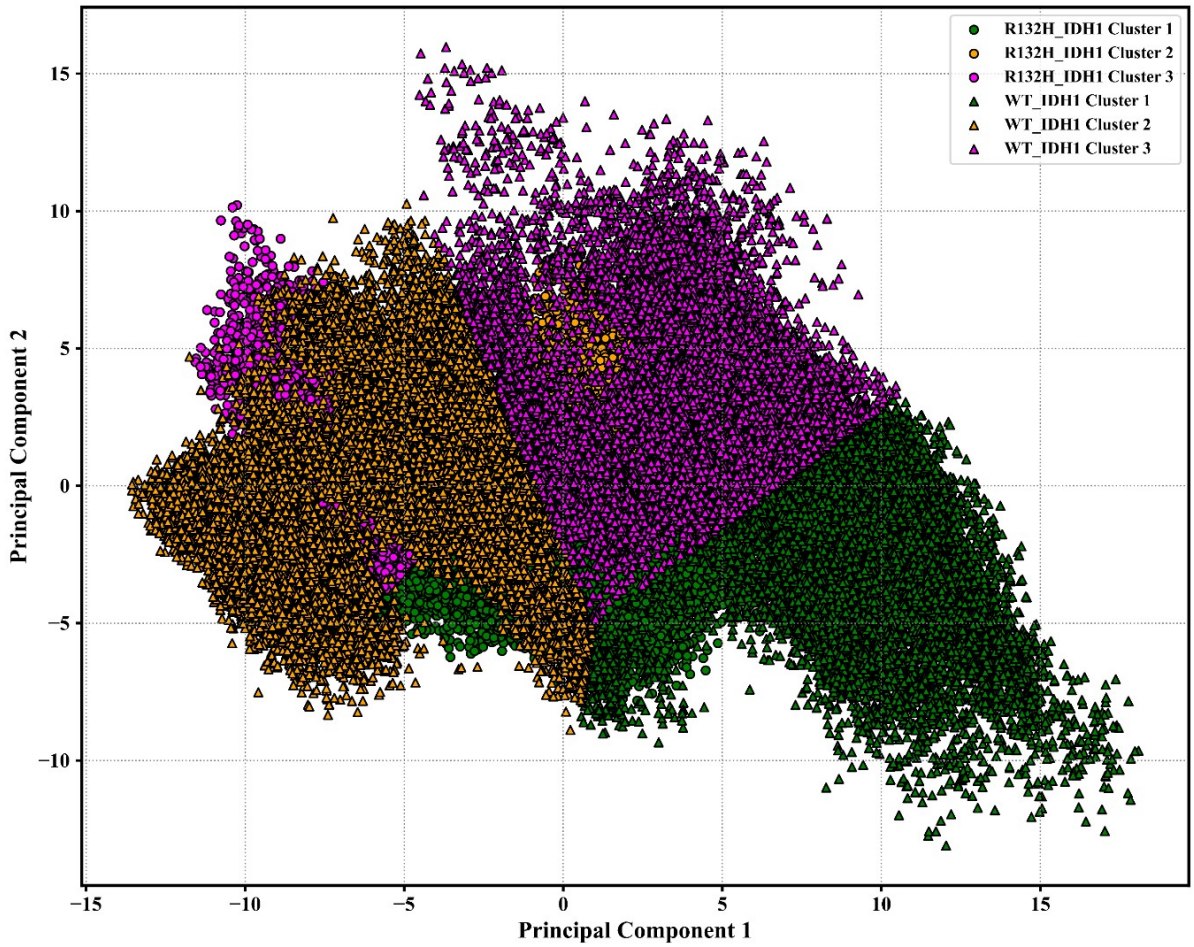
R132H_IDH1 Cluster 1
R132H_IDH1 Cluster 2
R132H_IDH1 Cluster 3
WT_IDH1 Cluster 1
WT_IDH1 Cluster 2
WT_IDH1 Cluster 3
Principal Component 2
Principal Component 1
15
10
5
0
−5
−10
−15
−10
−5
0
5
10
15

B

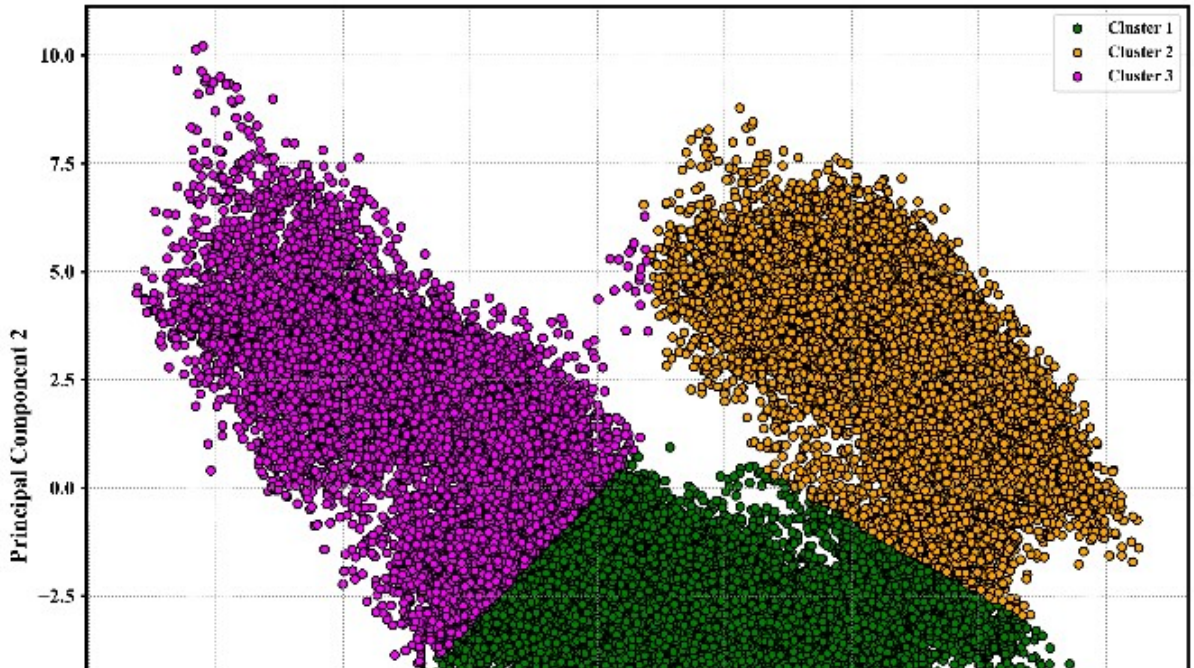
Cluster 1
Cluster 2
Cluster 3
Principal Component 2
10.0
7.5
5.0
2.5
0.0
−2.5

C

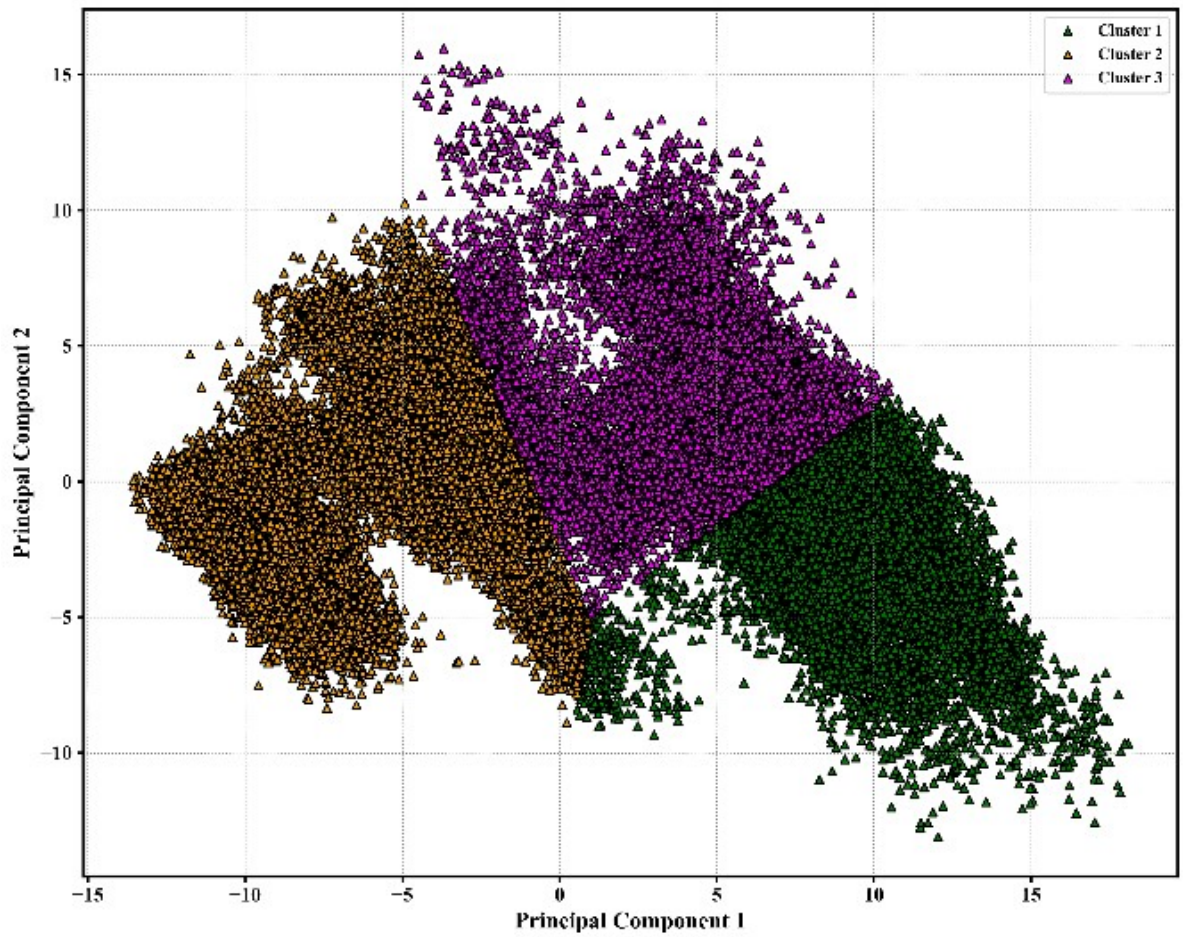
Cluster 1
Cluster 2
Cluster 3
Principal Component 2
Principal Component 1
15
10
5
0
−5
−10
−15
−10
−5
0
5
10
15

D

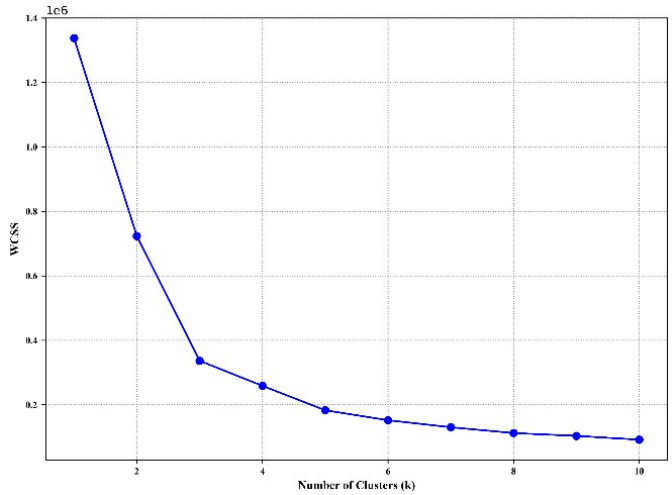
1e6
WCSS
Number of Clusters (k)
1.4
1.2
1.0
0.8
0.6
0.4
0.2
2
4
6
8
10

E

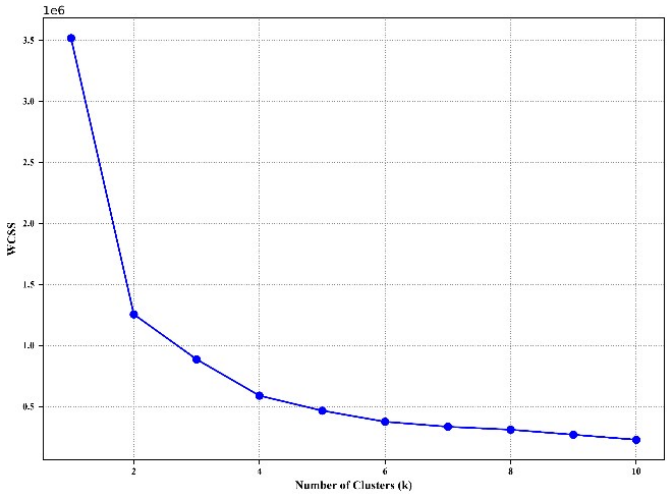
1e6
WCSS
Number of Clusters (k)
3.5
3.0
2.5
2.0
1.5
1.0
0.5
2
4
6
8
10

F

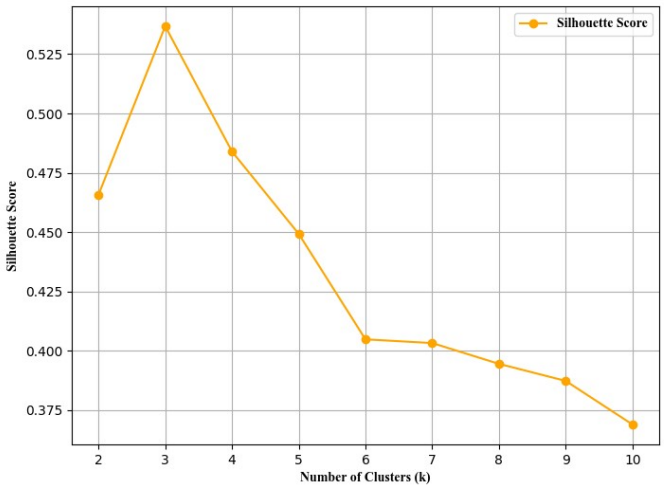


G

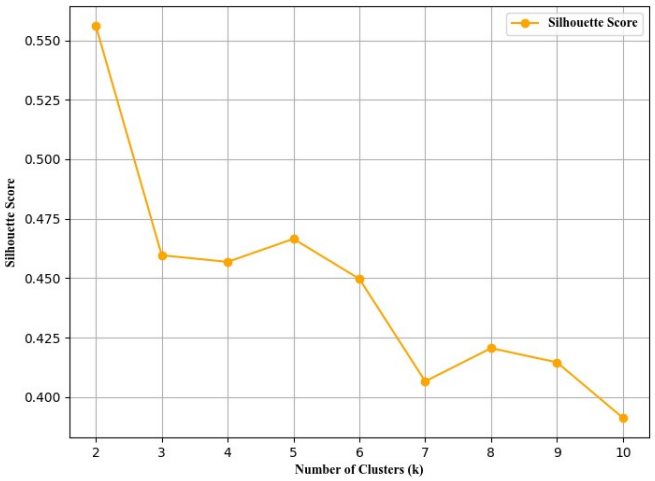


**Figure S8.** Cluster plot of PC1 vs PC2 for (A) comparing conformational space of R132H_IDH1 and WT_IDH1, (B) conformational space of R132H_IDH1, (C) conformational space of WT_IDH1, Elbow plot for (D) R132H_IDH1, (E) WT_IDH1, and Silhouette plot for (F) R132H_IDH1, (G) WT_IDH1 at pH 7.2.

A

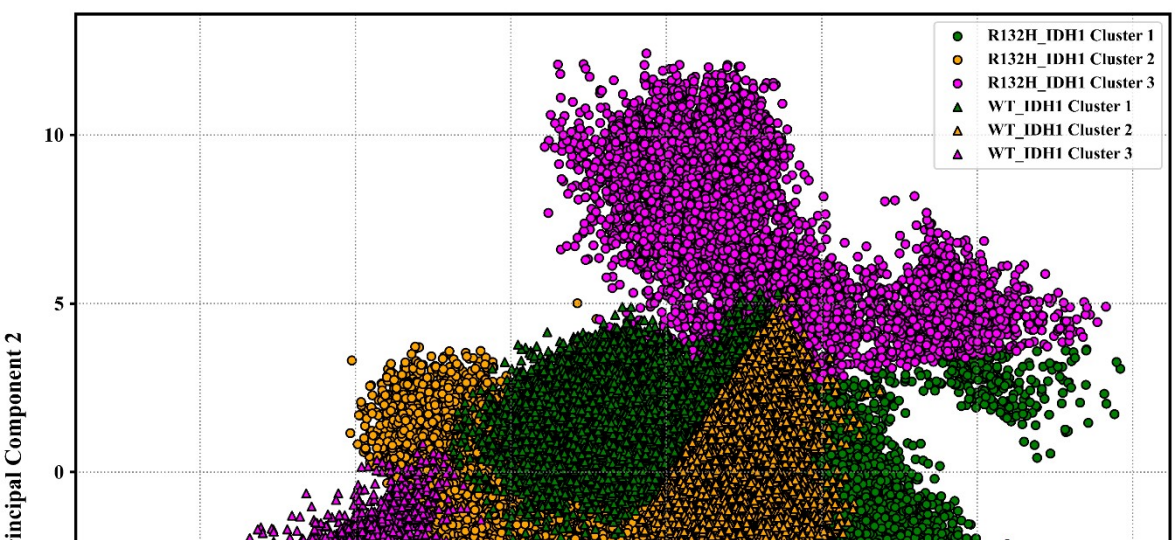

B

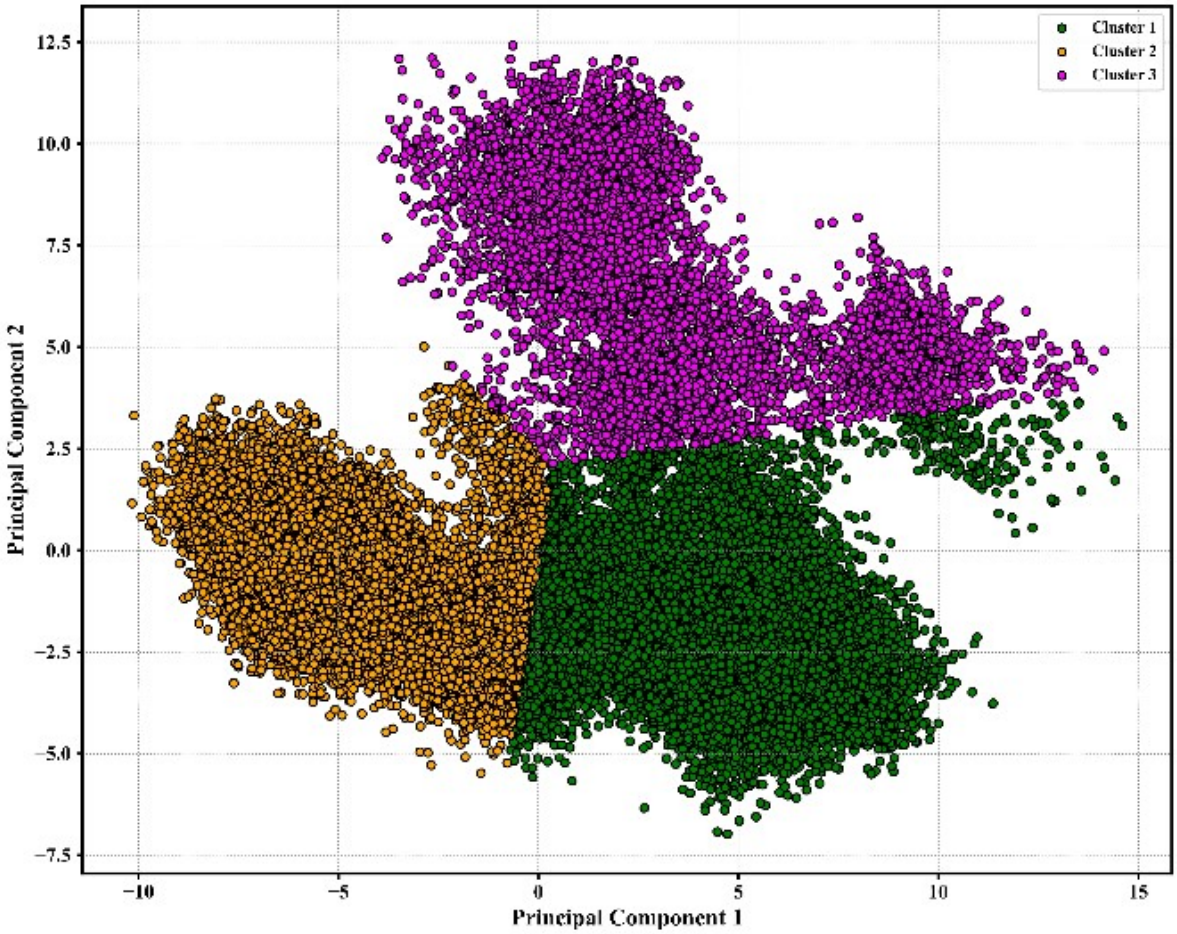
Cluster 1
Cluster 2
Cluster 3
Principal Component 2
Principal Component 1
12.5
10.0
7.5
5.0
2.5
0.0
−2.5
−5.0
−7.5
−10
−5
0
5
10
15

C

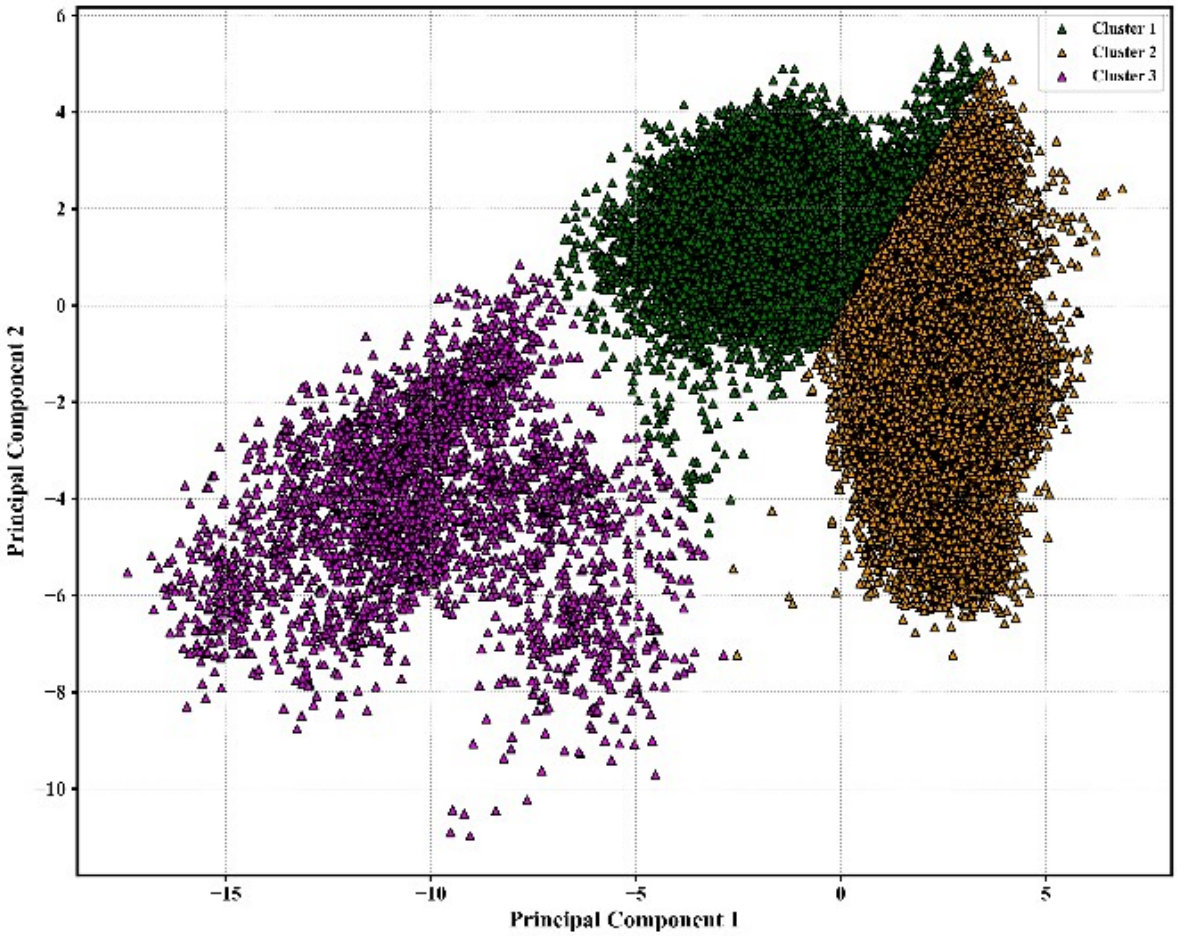
Cluster 1
Cluster 2
Cluster 3
Principal Component 2
Principal Component 1
6
4
2
0
−2
−4
−6
−8
−10
−15
−10
−5
0
5

D

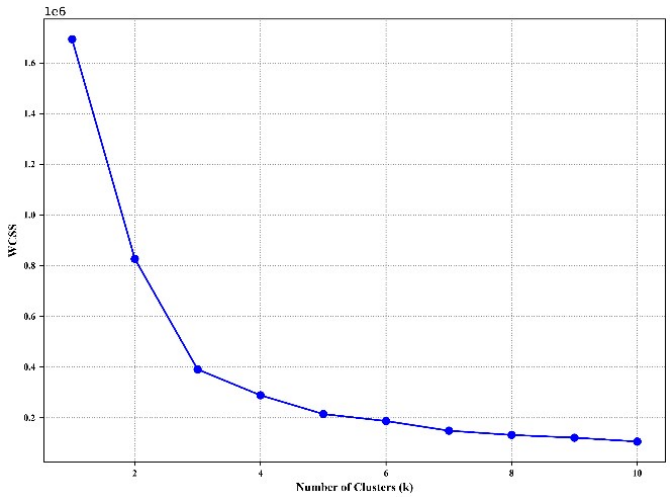


E

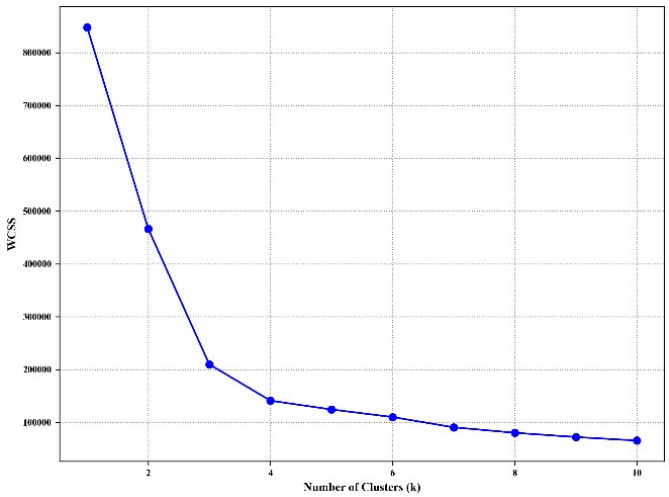


F

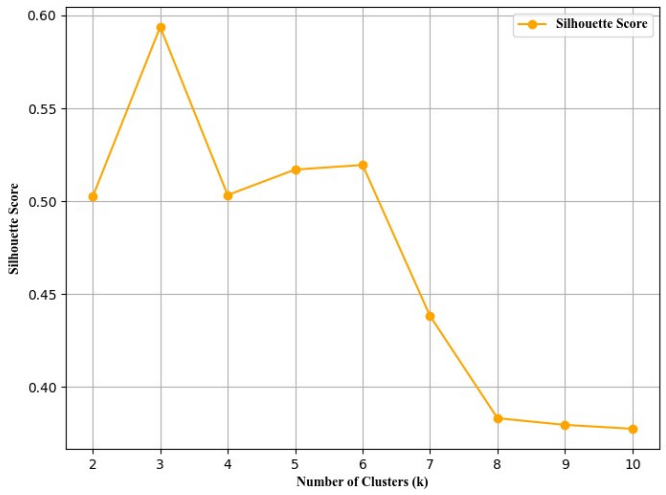


G

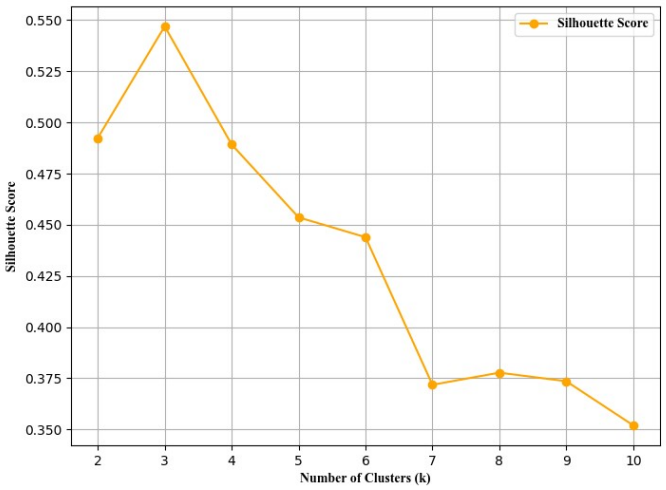


**Figure S9**. Cluster plot of PC1 vs PC2 for (A) comparing conformational space of R132H_IDH1 and WT_IDH1, (B) conformational space of R132H_IDH1, (C) conformational space of WT_IDH1, Elbow plot for (D) R132H_IDH1, (E) WT_IDH1, and Silhouette plot for (F) R132H_IDH1, (G) WT_IDH1 at pH 6.8.

A

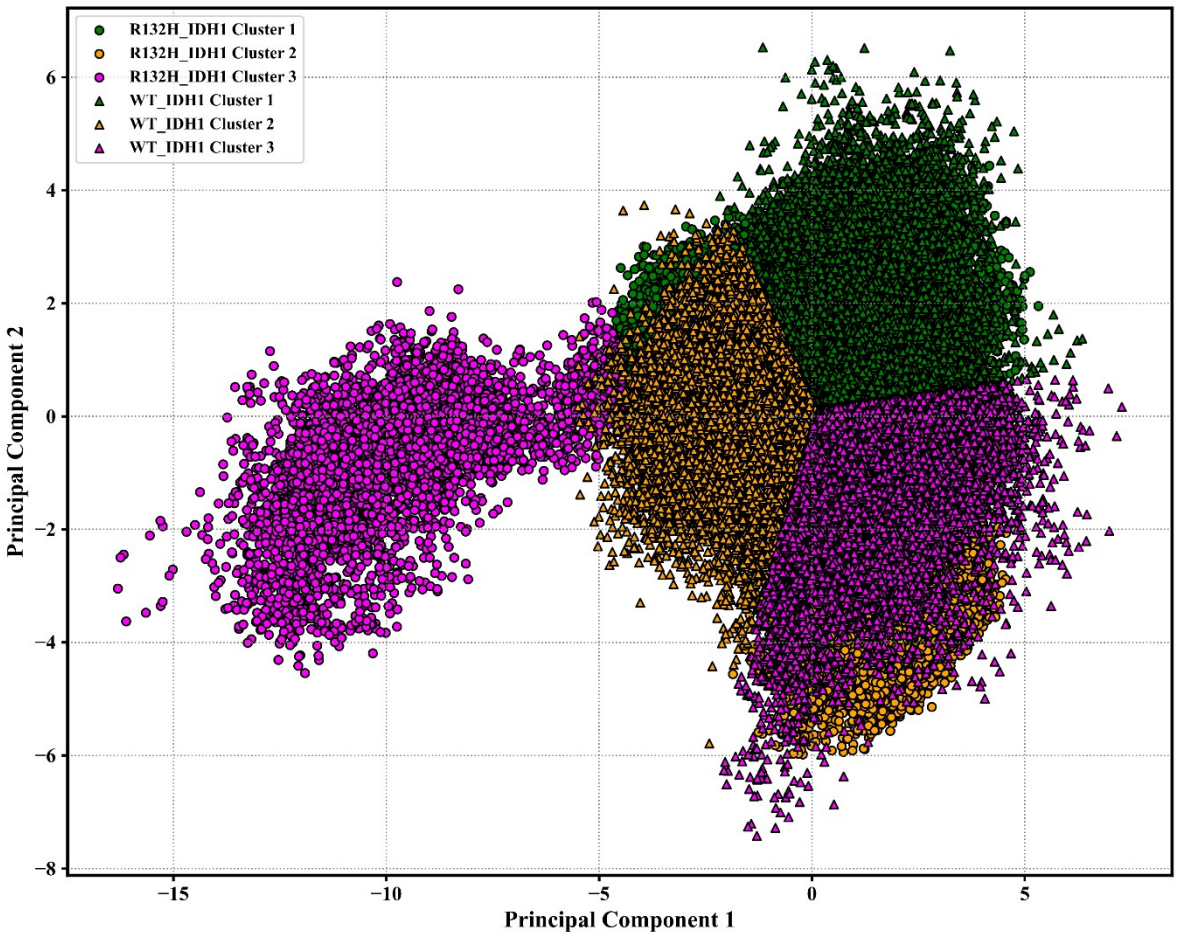
R132H_IDH1 Cluster 1
R132H_IDH1 Cluster 2
R132H_IDH1 Cluster 3
WT_IDH1 Cluster 1
WT_IDH1 Cluster 2
WT_IDH1 Cluster 3
Principal Component 2
Principal Component 1
6
4
2
0
−2
−4
−6
−8
−15
−10
−5
0
5

B

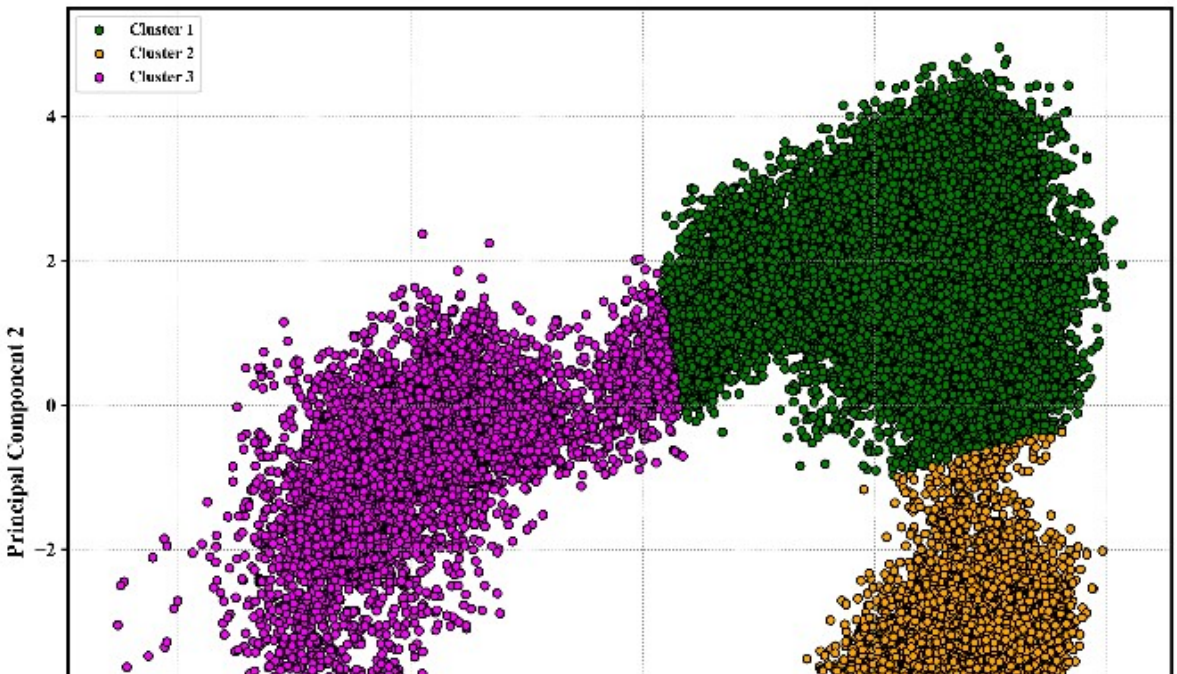
Cluster 1
Cluster 2
Cluster 3
Principal Component 2
4
2
0
−2

C

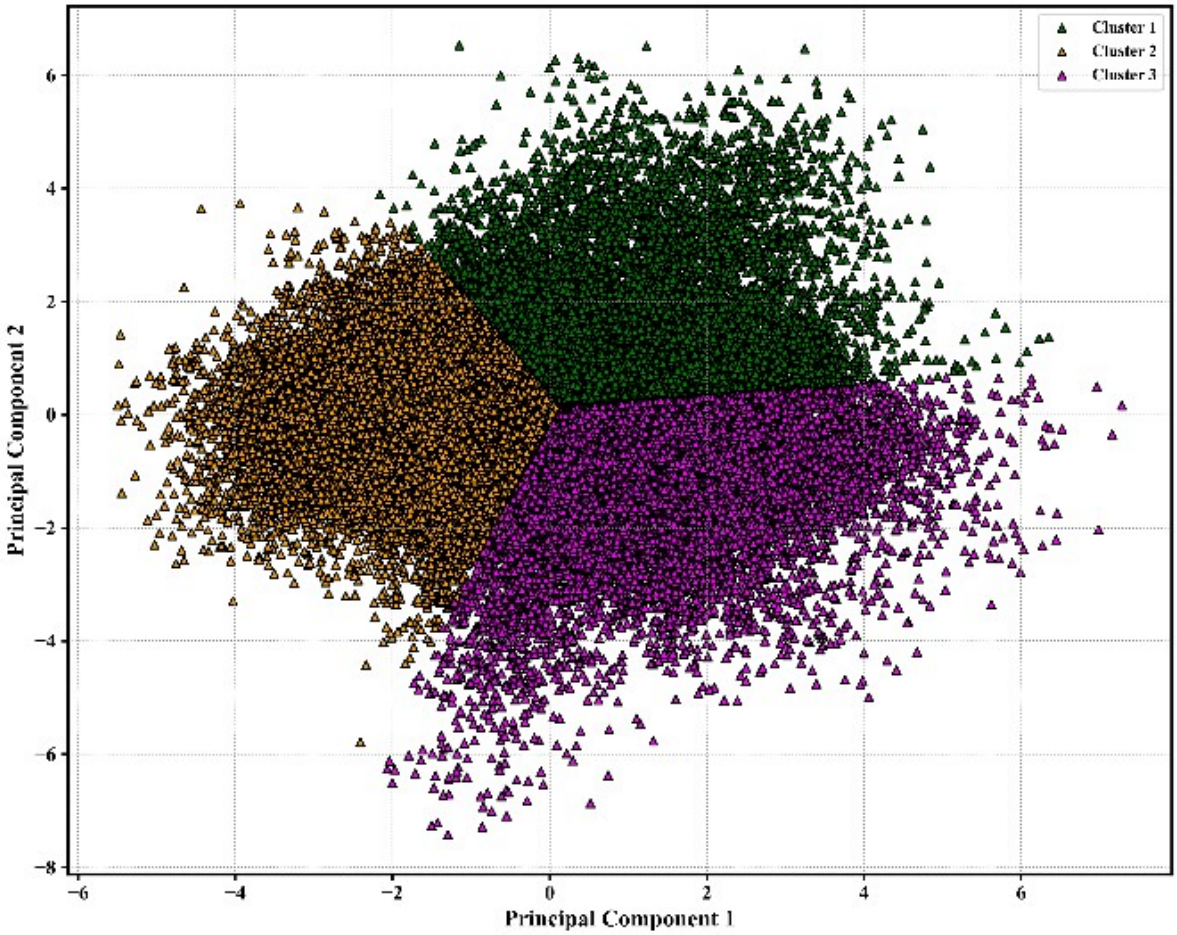
Cluster 1
Cluster 2
Cluster 3
Principal Component 2
Principal Component 1

D

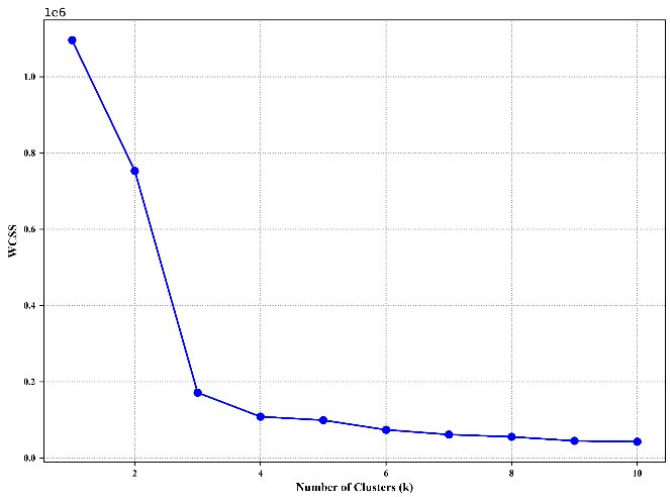
1e6
WCSS
Number of Clusters (k)

E

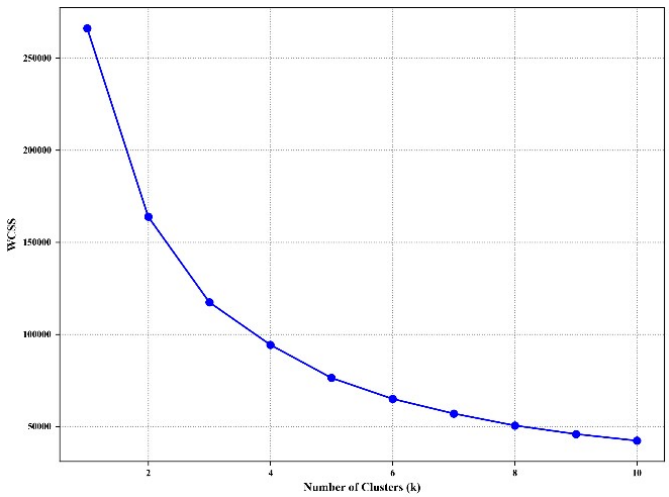
WCSS
Number of Clusters (k)

F

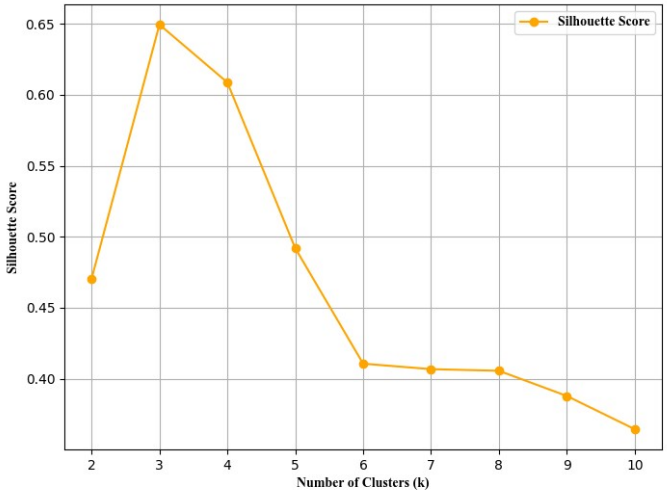


G

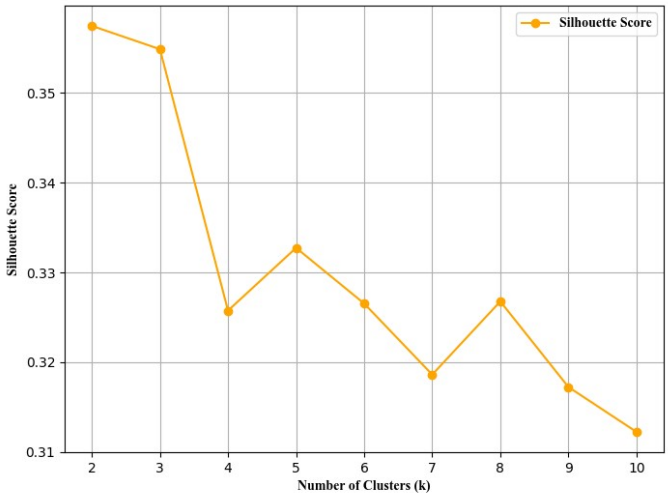


**Figure S10.** Cluster plot of PC1 vs PC2 for (A) comparing conformational space of R132H_IDH1 and WT_IDH1, (B) conformational space of R132H_IDH1, (C) conformational space of WT_IDH1, Elbow plot for (D) R132H_IDH1, (E) WT_IDH1, and Silhouette plot for (F) R132H_IDH1 (G) WT_IDH1 at pH 5.6.

A

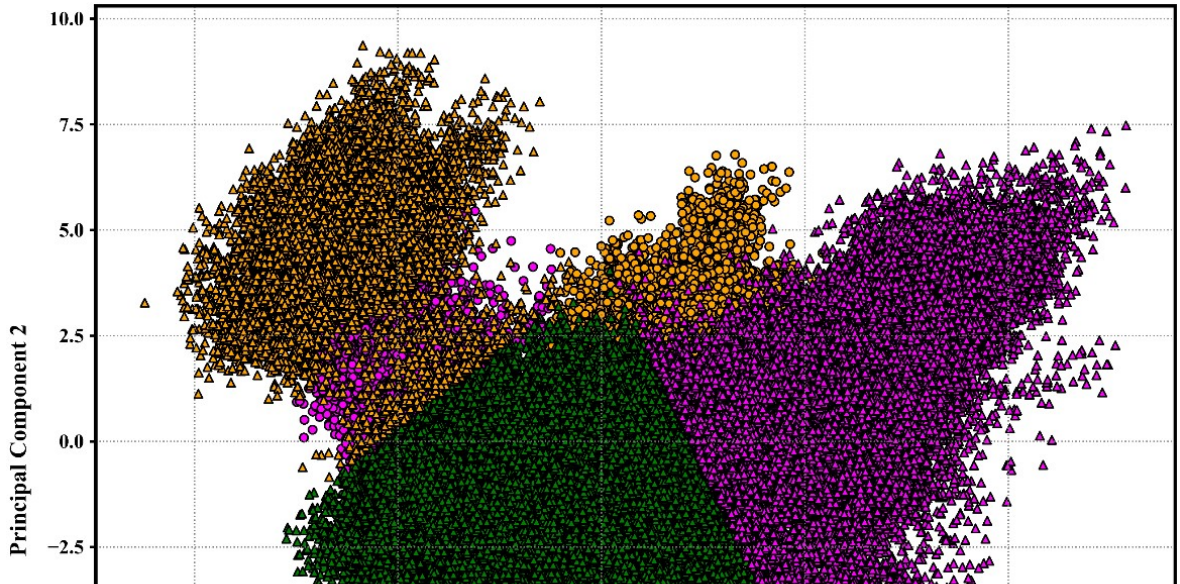

B

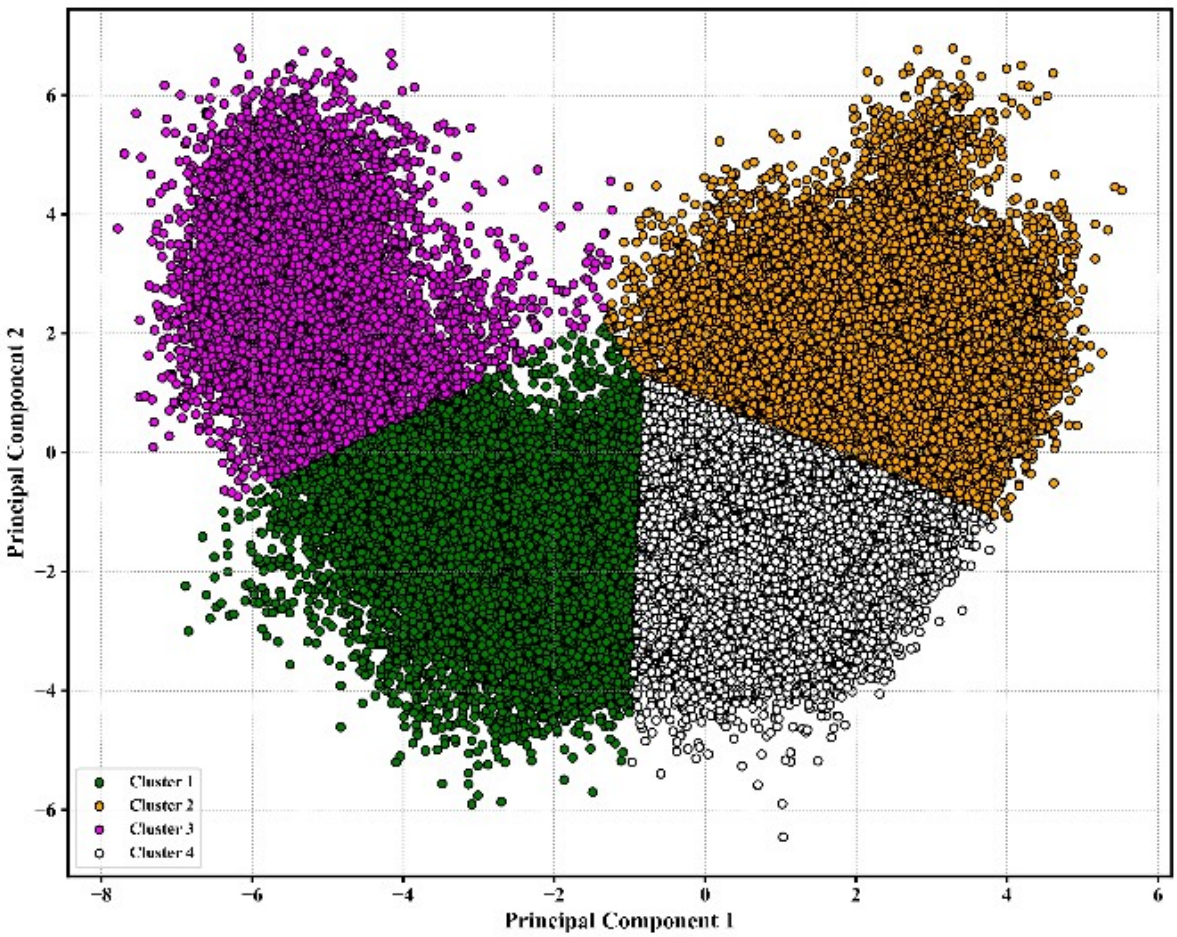
Principal Component 2
Principal Component 1
Cluster 1
Cluster 2
Cluster 3
Cluster 4

C

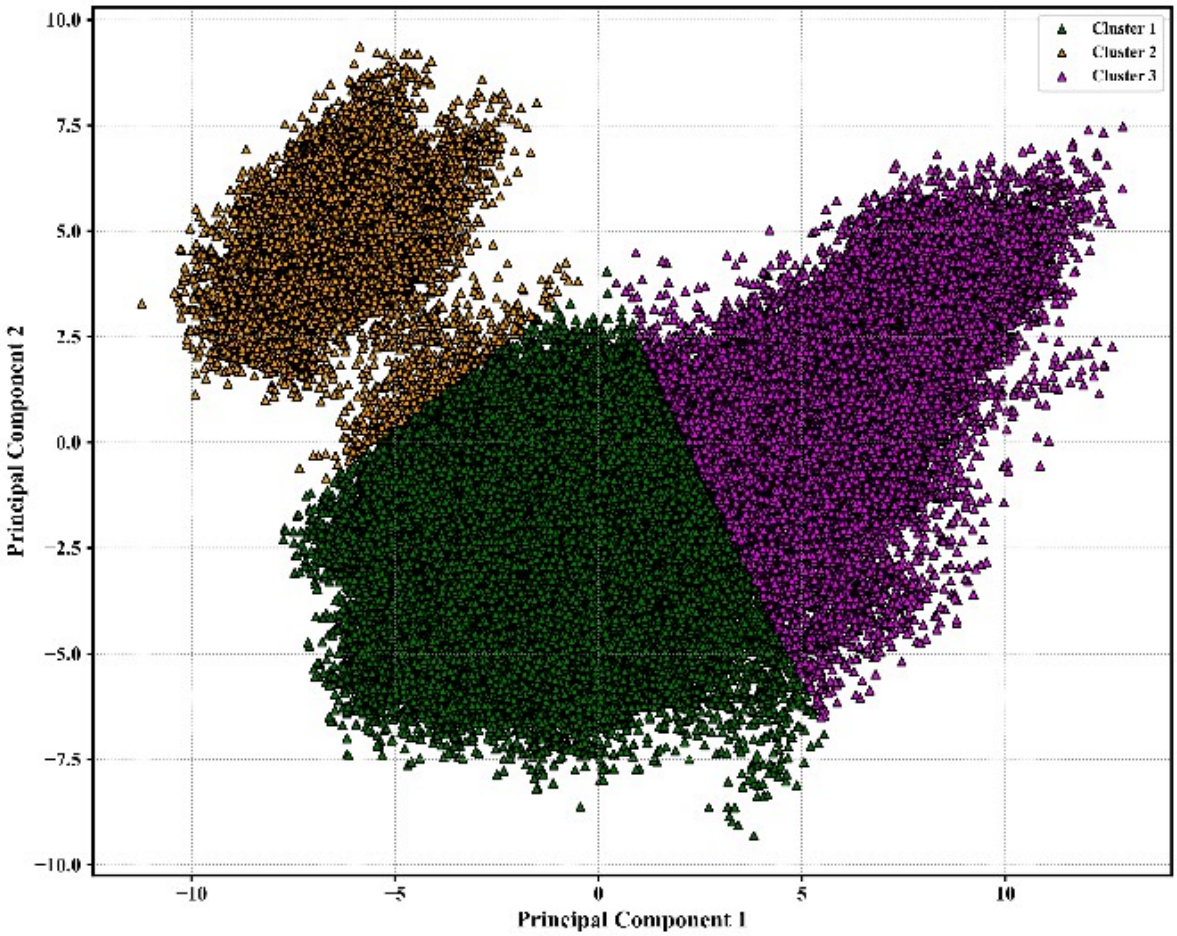
Principal Component 2
Principal Component 1
Cluster 1
Cluster 2
Cluster 3

D E

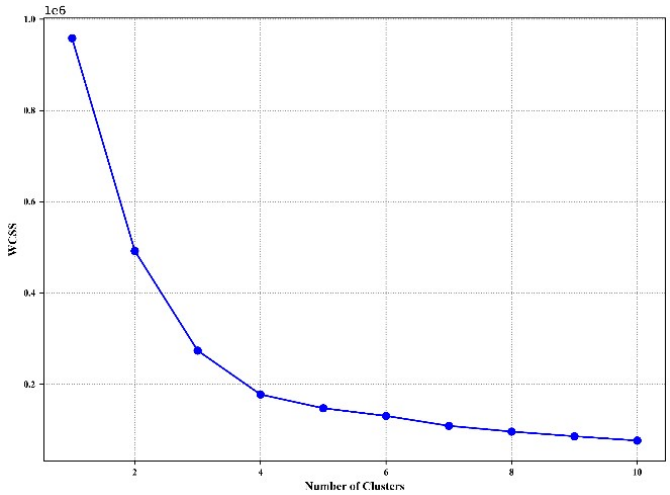
1e6
WCSS
Number of Clusters

F

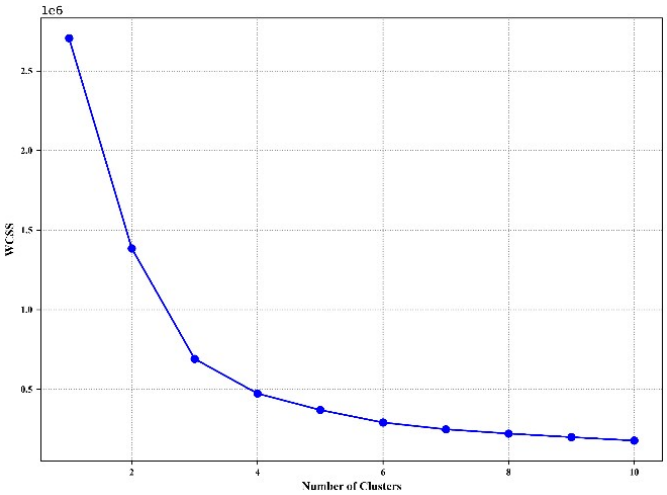
1e6
WCSS
Number of Clusters

G

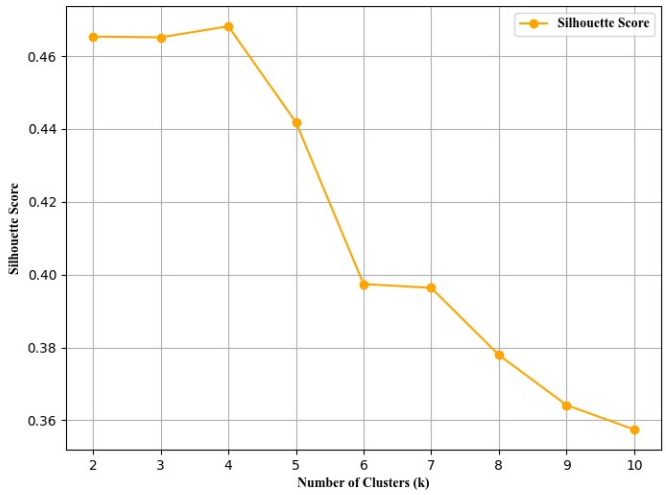
Silhouette Score
Silhouette Score
Number of Clusters (k)

H

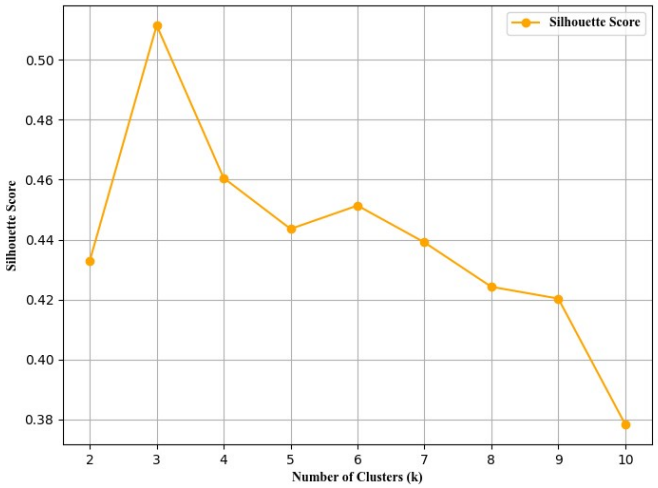
Silhouette Score
Silhouette Score
Number of Clusters (k)

I

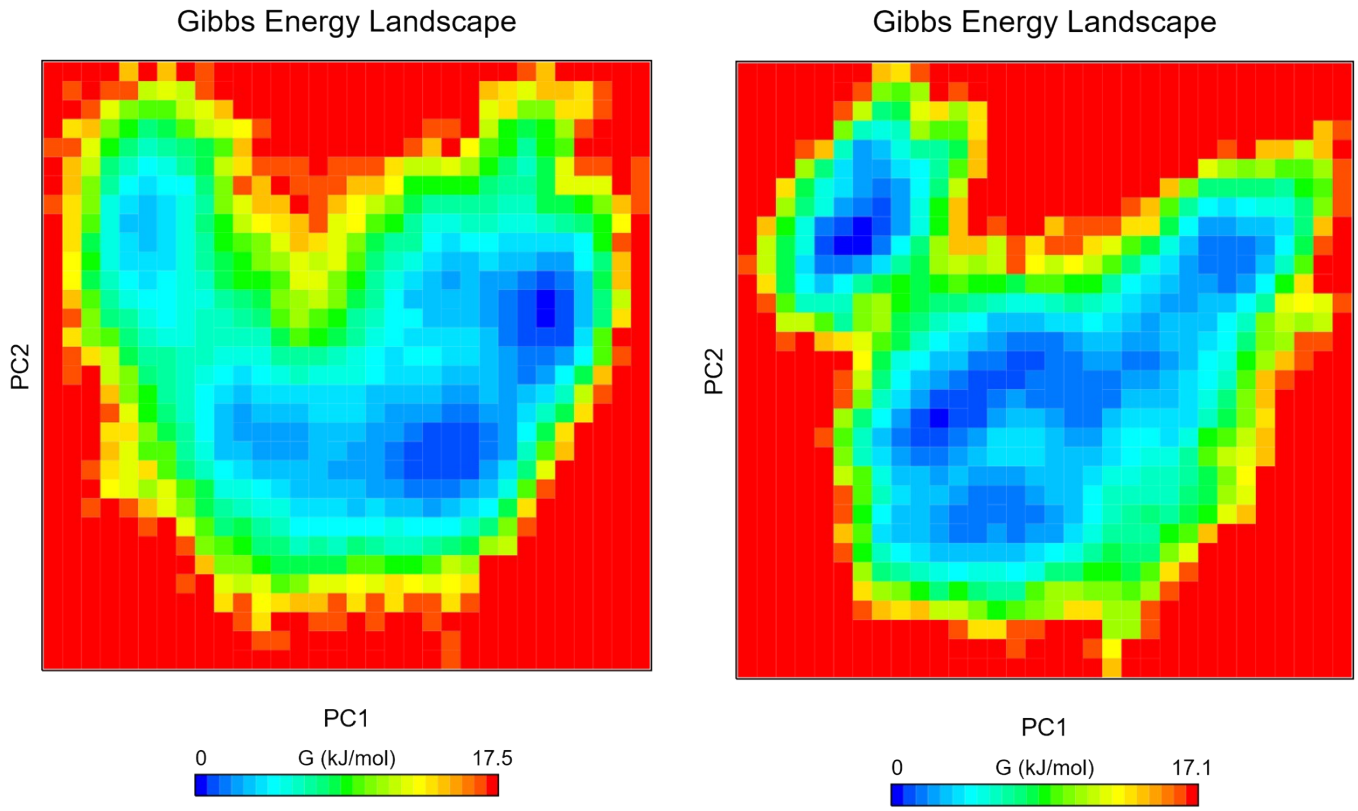


**Figure S11.** Cluster plot of PC1 vs PC2 for (A) comparing conformational space of ICT bound R132H_IDH1 and WT_IDH1 (B) conformational space of ICT bound R132H_IDH1 (C) conformational space of ICT bound WT_IDH1, elbow plot for (D) ICT bound R132H_IDH1 (E) ICT bound WT_IDH1, and Silhouette plot for (F) ICT bound R132H_IDH1 (G) ICT bound WT_IDH1 (H) FEL of ICT bound R132H_IDH1 and (I) FEL of ICT bound WT_IDH1at pH 7.4.

A

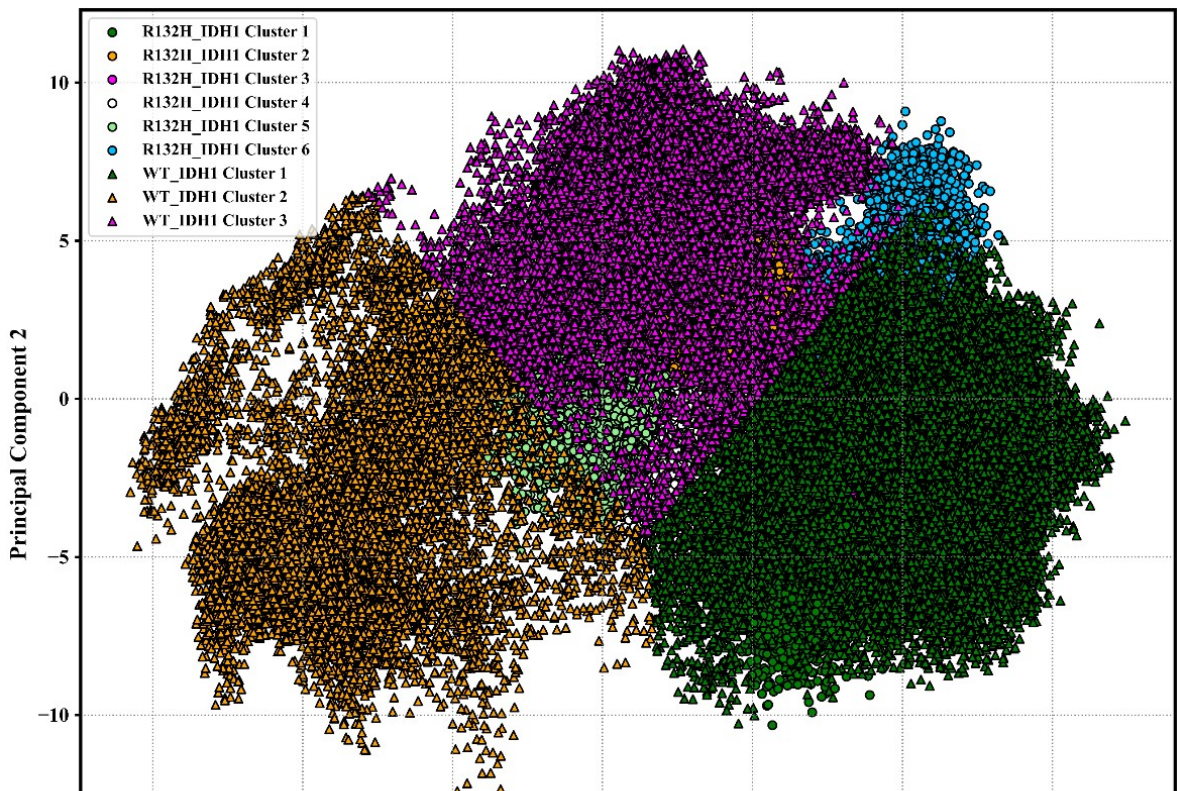

B

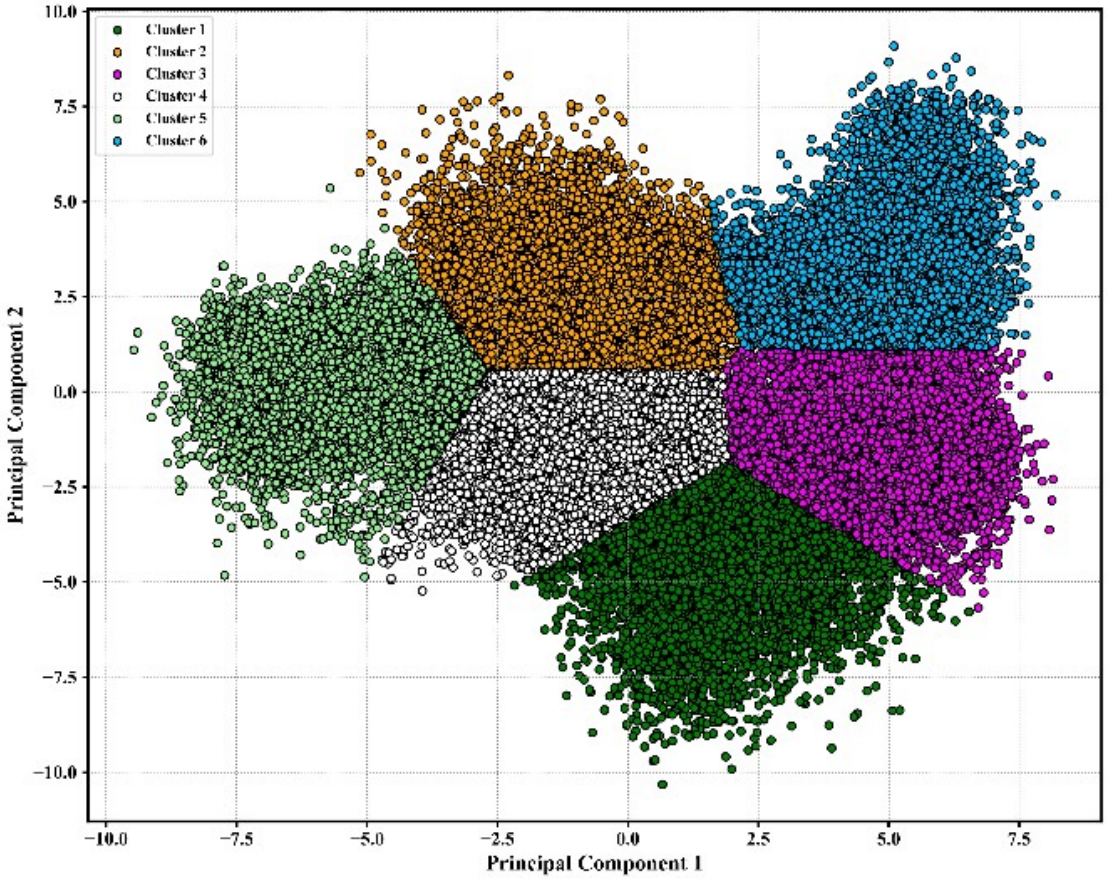
Cluster 1
Cluster 2
Cluster 3
Cluster 4
Cluster 5
Cluster 6
Principal Component 2
Principal Component 1
10.0
7.5
5.0
2.5
0.0
−2.5
−5.0
−7.5
−10.0
−10.0
−7.5
−5.0
−2.5
0.0
2.5
5.0
7.5

C

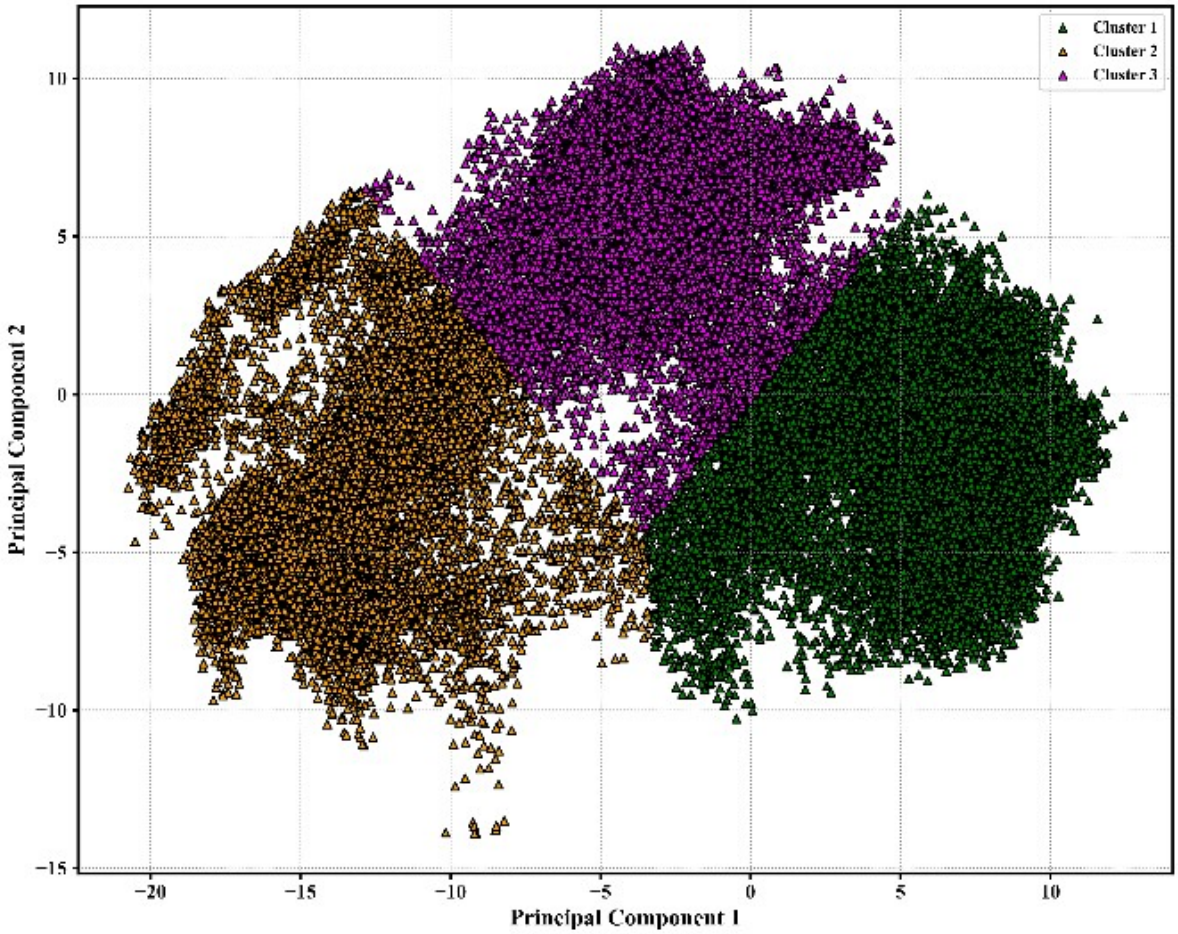
Cluster 1
Cluster 2
Cluster 3
Principal Component 2
Principal Component 1
10
5
0
−5
−10
−15
−20
−15
−10
−5
0
5
10

D

E

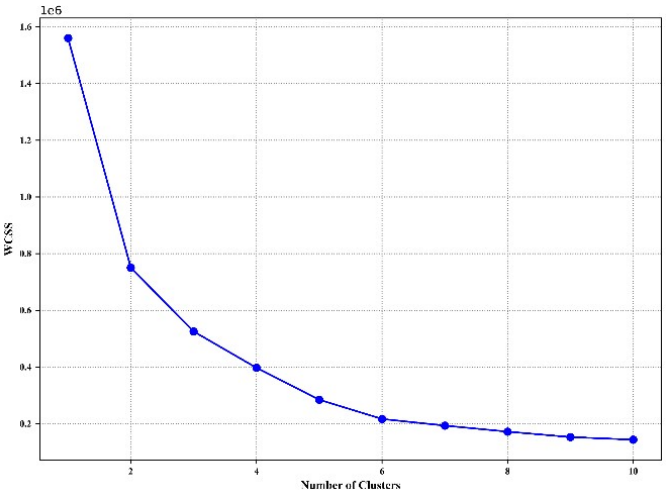
1e6
WCSS
Number of Clusters
1.6
1.4
1.2
1.0
0.8
0.6
0.4
0.2
2
4
6
8
10

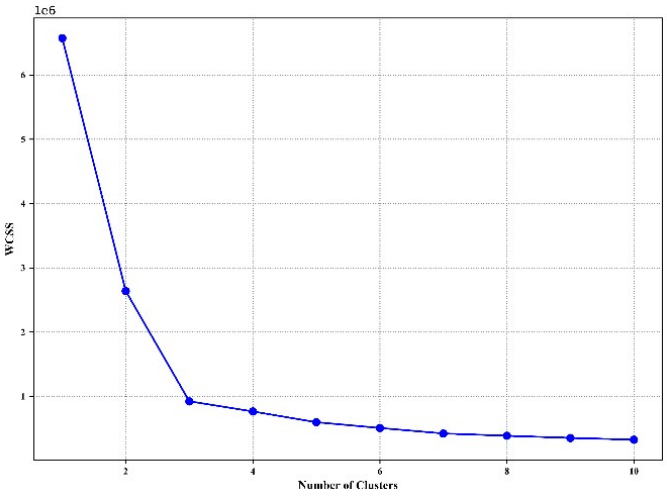
1e6
WCSS
Number of Clusters
6
5
4
3
2
1
2
4
6
8
10

F

G

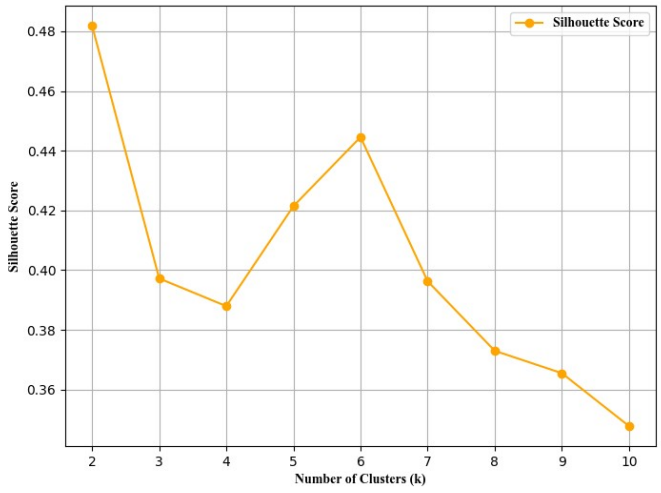


H

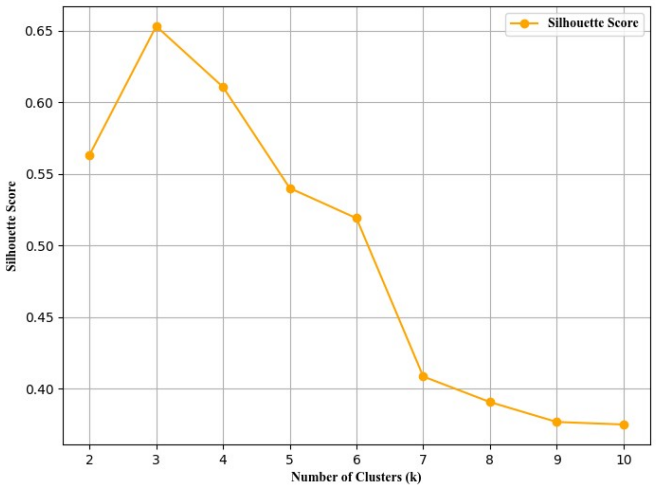


I

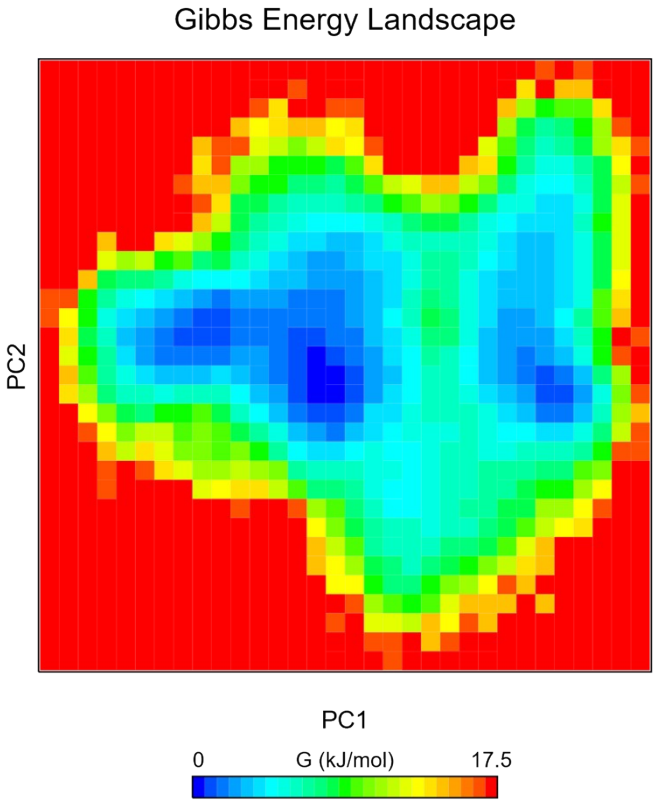


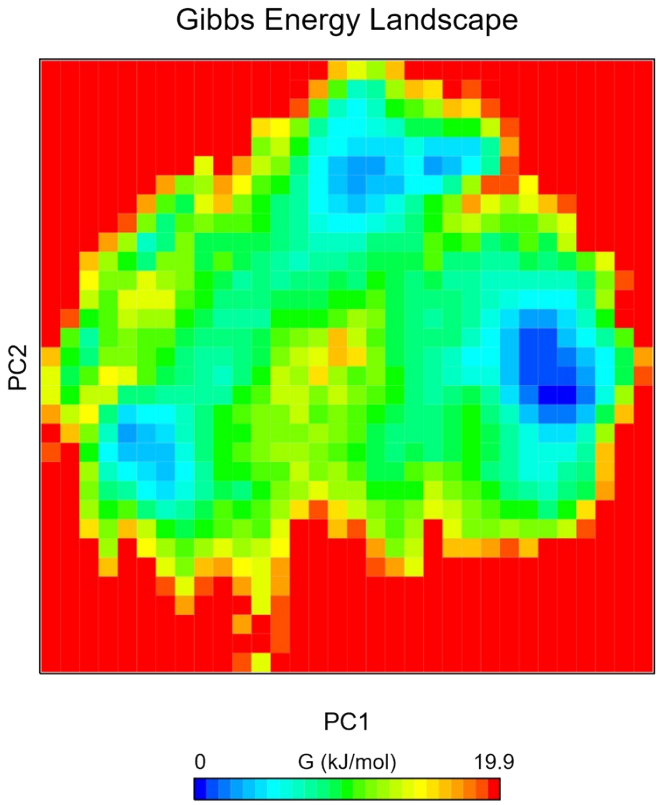


**Figure S12.** Cluster plot of PC1 vs PC2 for (A) comparing conformational space of NADPH bound R132H_IDH1 and WT_IDH1 (B) conformational space of NADPH bound R132H_IDH1 (C) conformational space of NADPH bound WT_IDH1, elbow plot for (D) NADPH bound R132H_IDH1 (E) NADPH bound WT_IDH1, and Silhouette plot for (F) NADPH bound R132H_IDH1 (G) NADPH bound WT_IDH1 (H) FEL of NADPH bound R132H_IDH1 and (I) FEL of NADPH bound WT_IDH1at pH 7.4.

A

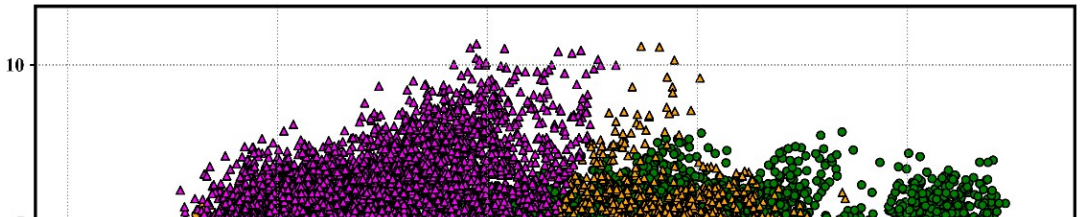

B

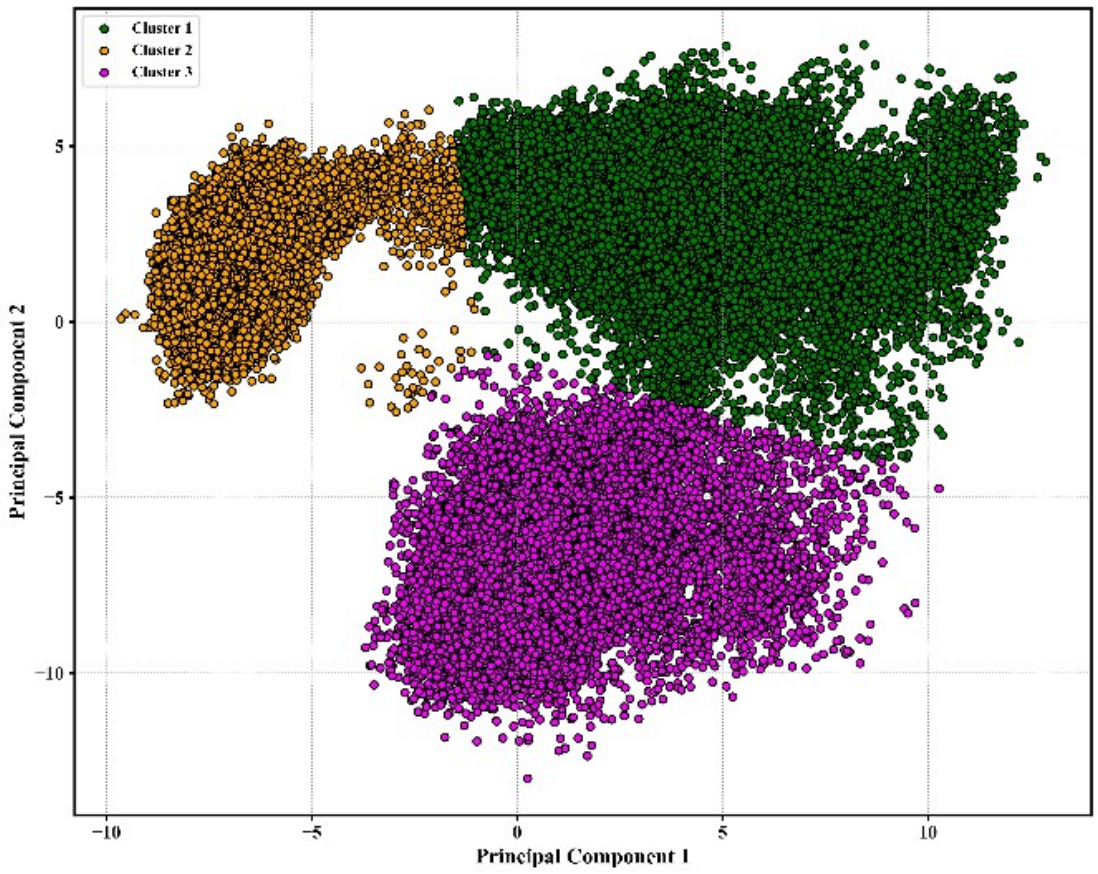
Cluster 1
Cluster 2
Cluster 3
Principal Component 2
Principal Component 1
5
0
−5
−10
−10
−5
0
5
10

C

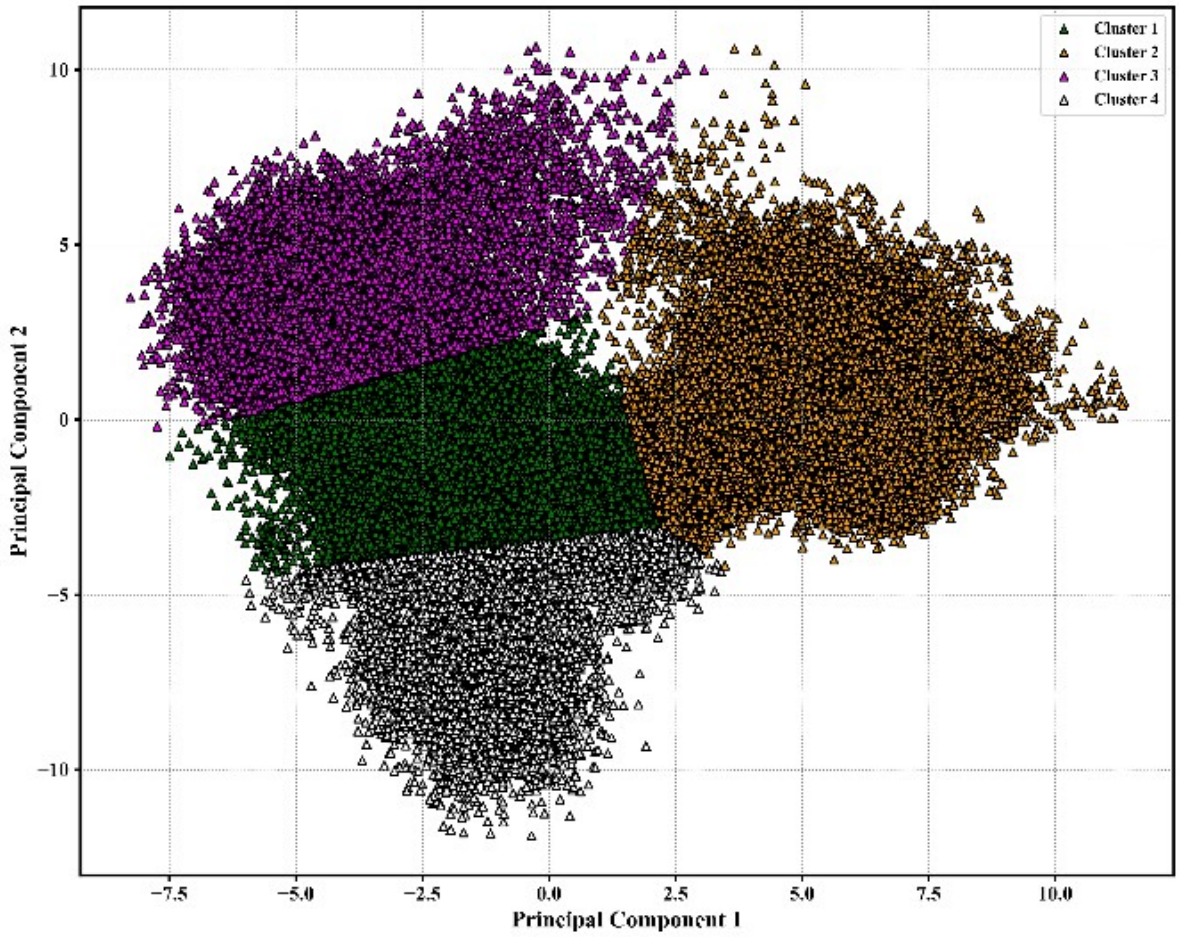
Cluster 1
Cluster 2
Cluster 3
Cluster 4
Principal Component 2
Principal Component 1
10
5
0
−5
−10
−7.5
−5.0
−2.5
0.0
2.5
5.0
7.5
10.0

D

E

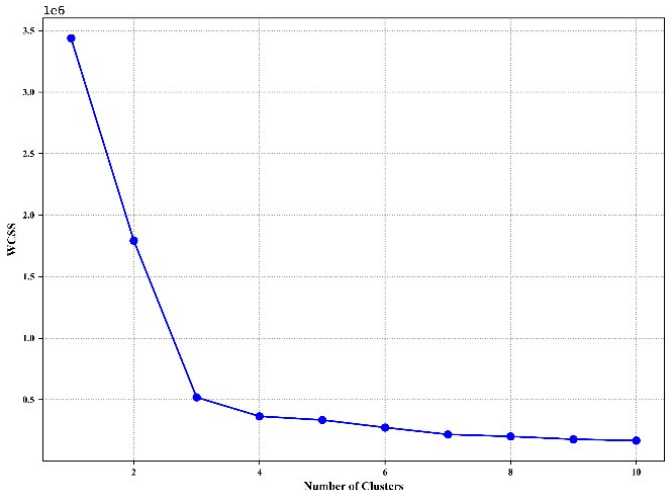
1e6
WCSS
Number of Clusters

F

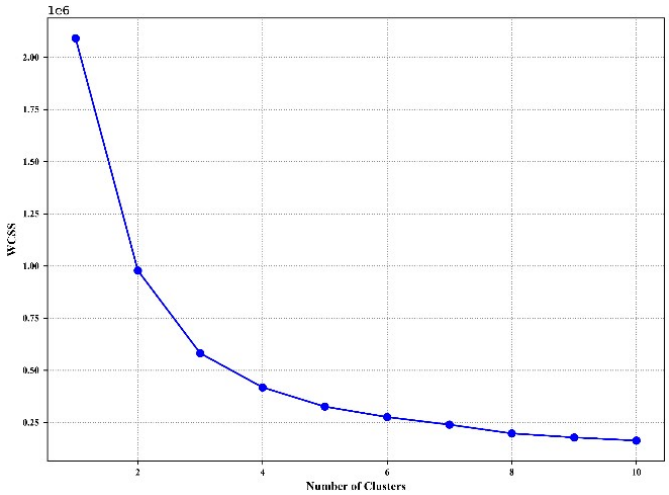
1e6
WCSS
Number of Clusters

G

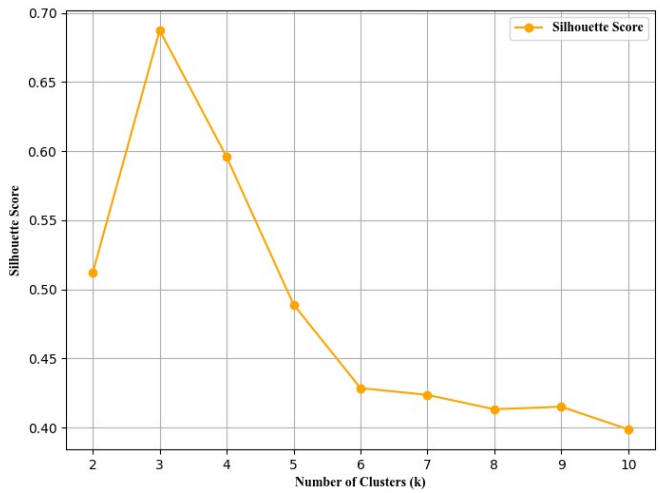
Silhouette Score
Silhouette Score
Number of Clusters (k)

H

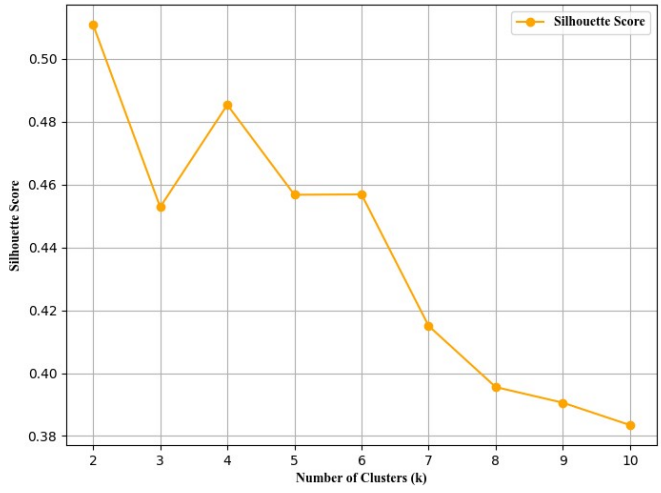
Silhouette Score
Silhouette Score
Number of Clusters (k)

I

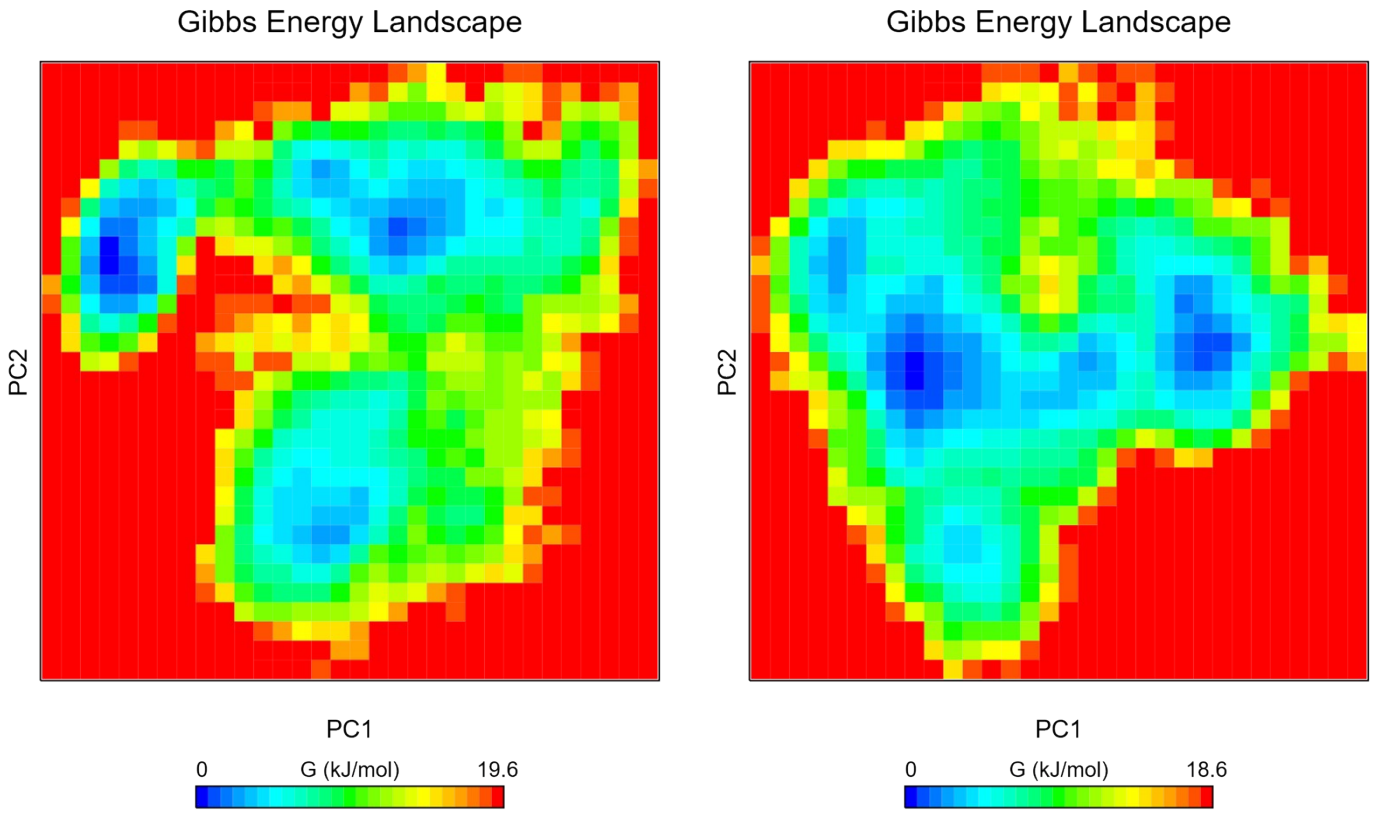


**Figure S13.** Cluster plot of PC1 vs PC2 for (A) comparing conformational space of ICT-NADPH bound R132H_IDH1 and WT_IDH1, (B) conformational space of ICT-NADPH bound R132H_IDH1 (C) conformational space of ICT-NADPH bound WT_IDH1, elbow plot for (D) ICT-NADPH bound R132H_IDH1 (E) ICT-NADPH bound WT_IDH1, and silhouette plot for (F) ICT-NADPH bound R132H_IDH1, (G) ICT-NADPH bound WT_IDH1 (H) FEL of ICT-NADPH bound R132H_IDH1, and (I) FEL of ICT-NADPH bound WT_IDH1at pH 7.4.

A

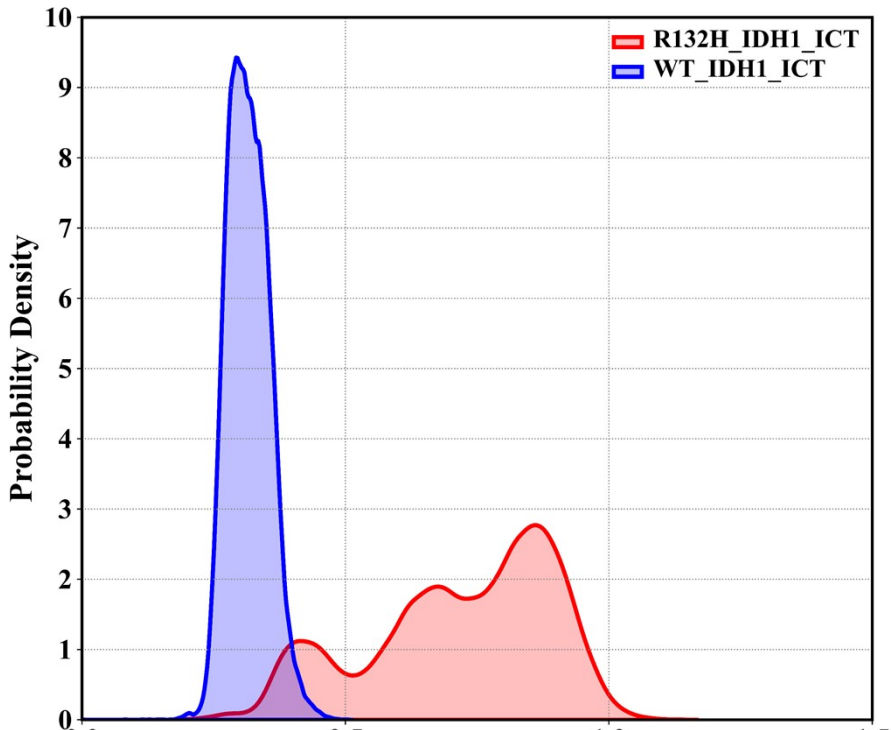

B

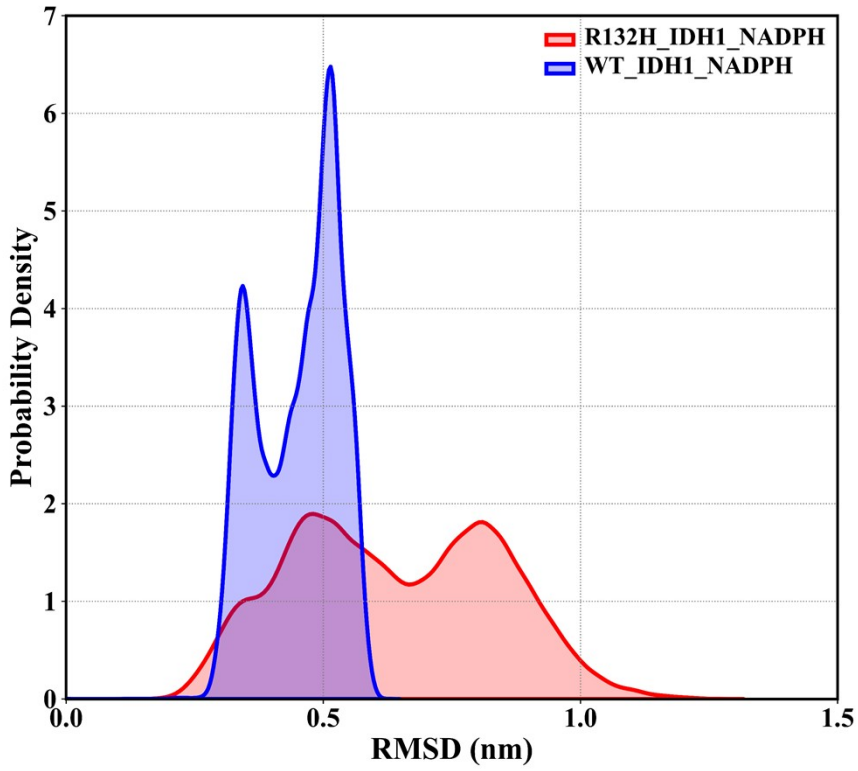


**Figure S14.** Distribution (kernel density estimation) of RMSD for segments $S_{12}$ for **(A)** R132H_IDH1_ICT and WT_IDH1_ICT and **(B)** R132H_IDH1_NADPH and WT_IDH1_NADPH.

A

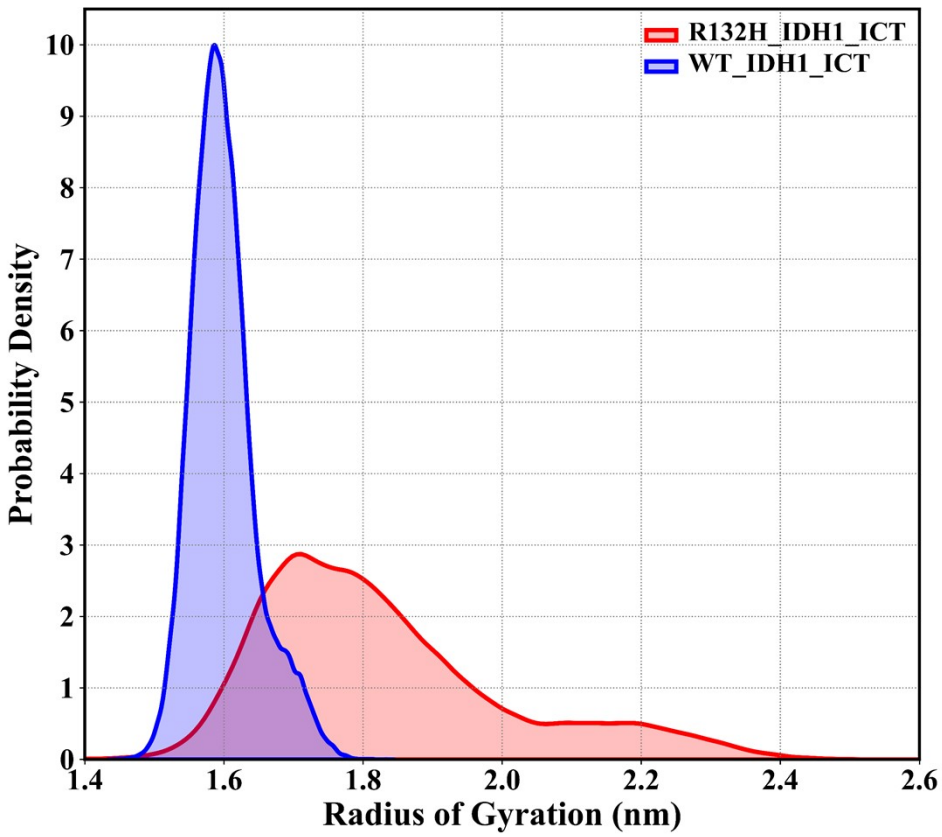

B

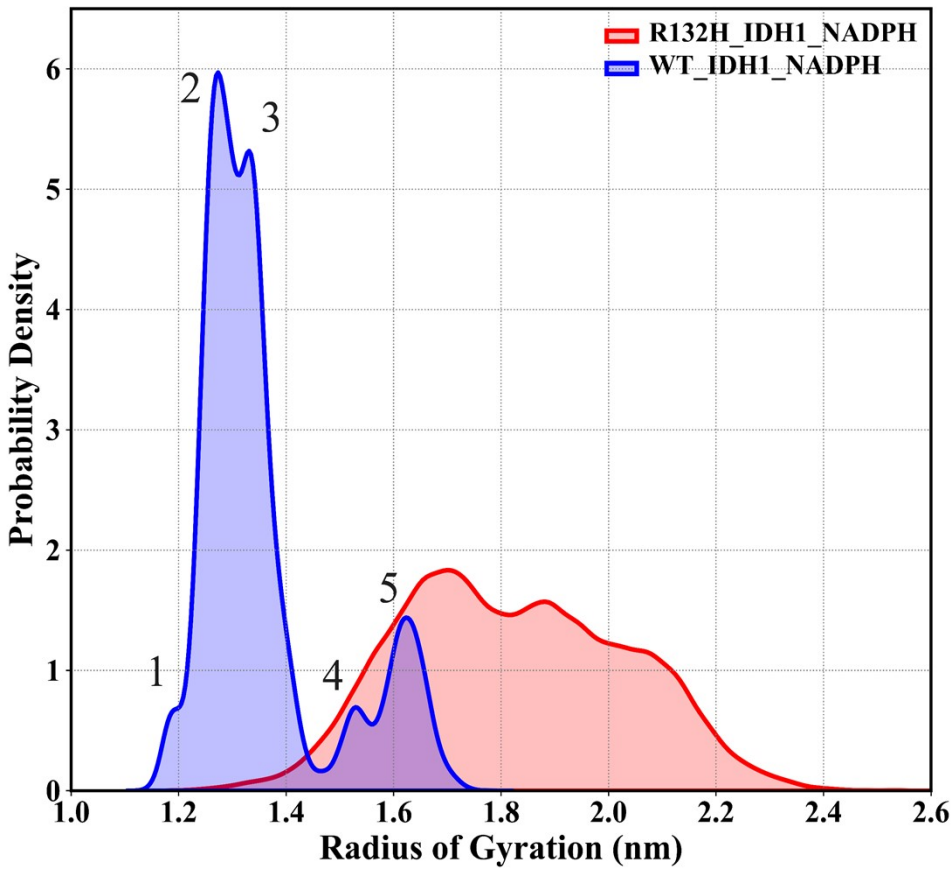


**Figure S15.** Distribution (kernel density estimation) of Rg for segments $S_{12}$ for (A) R132H_IDH1_ICT and WT_IDH1_ICT and (B) R132H_IDH1_NADPH and WT IDH1_NADPH.

A

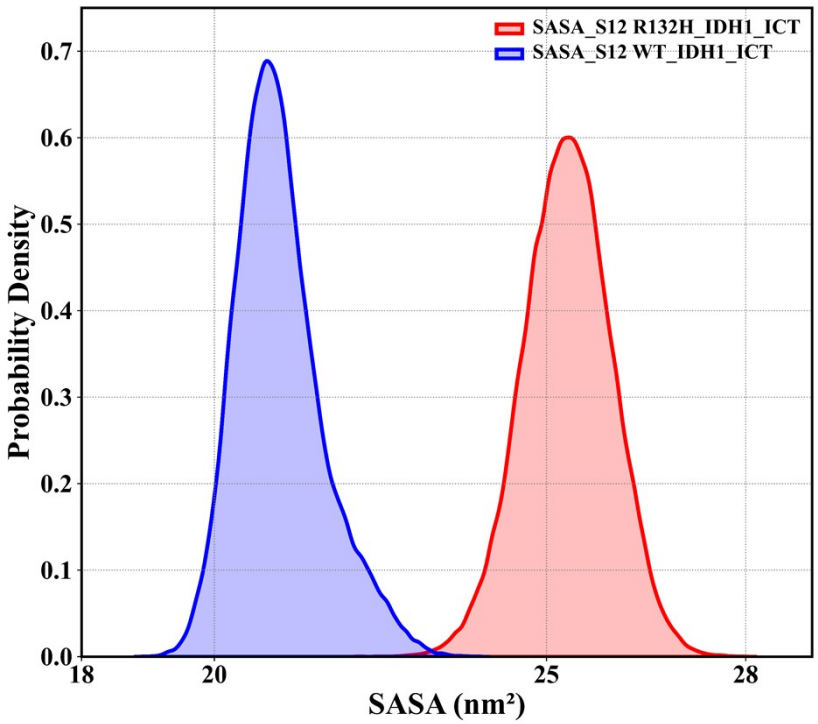


B

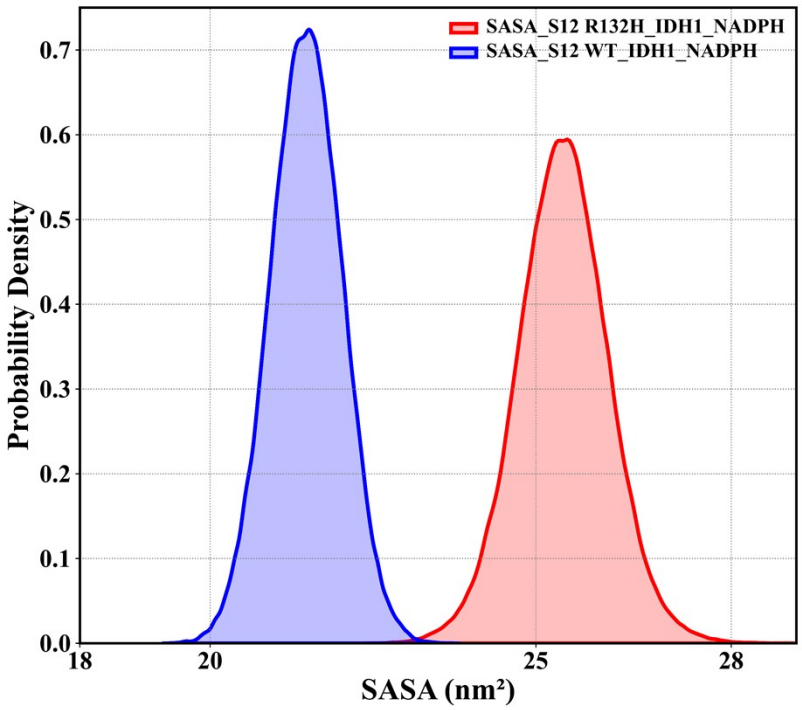


**Figure S16.** Distribution (kernel density estimation) of SASA ($nm^2$) for segments $S_{12}$ for **(A)** R132H_IDH1_ICT and WT_IDH1_ICT and **(B)** R132H_IDH1_NADPH and WT_IDH1_NADPH

A

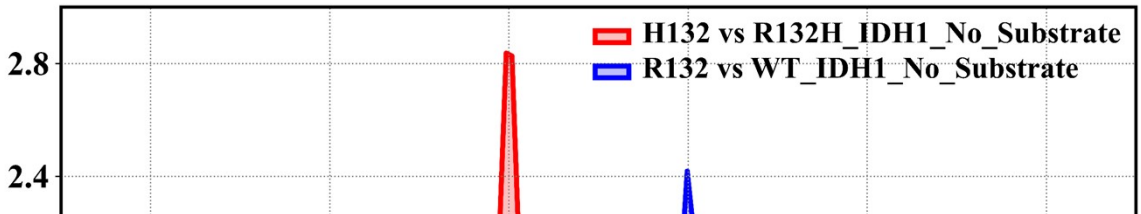

B

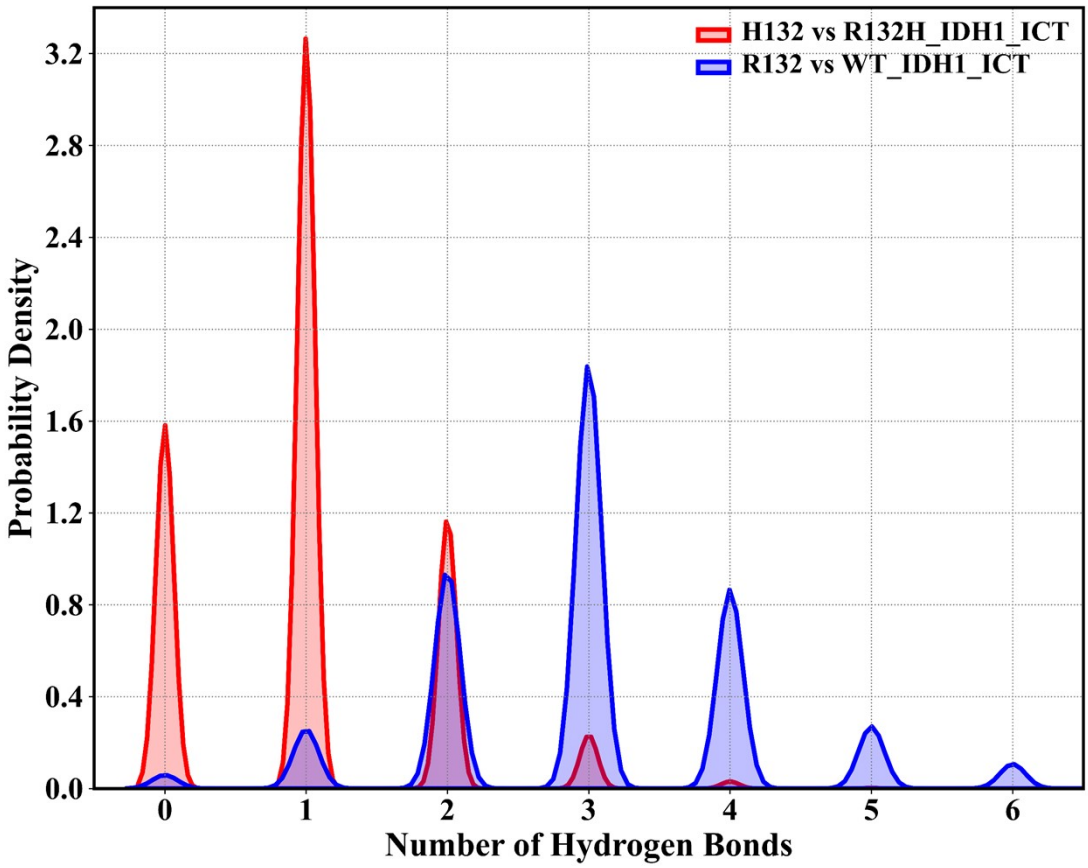


C

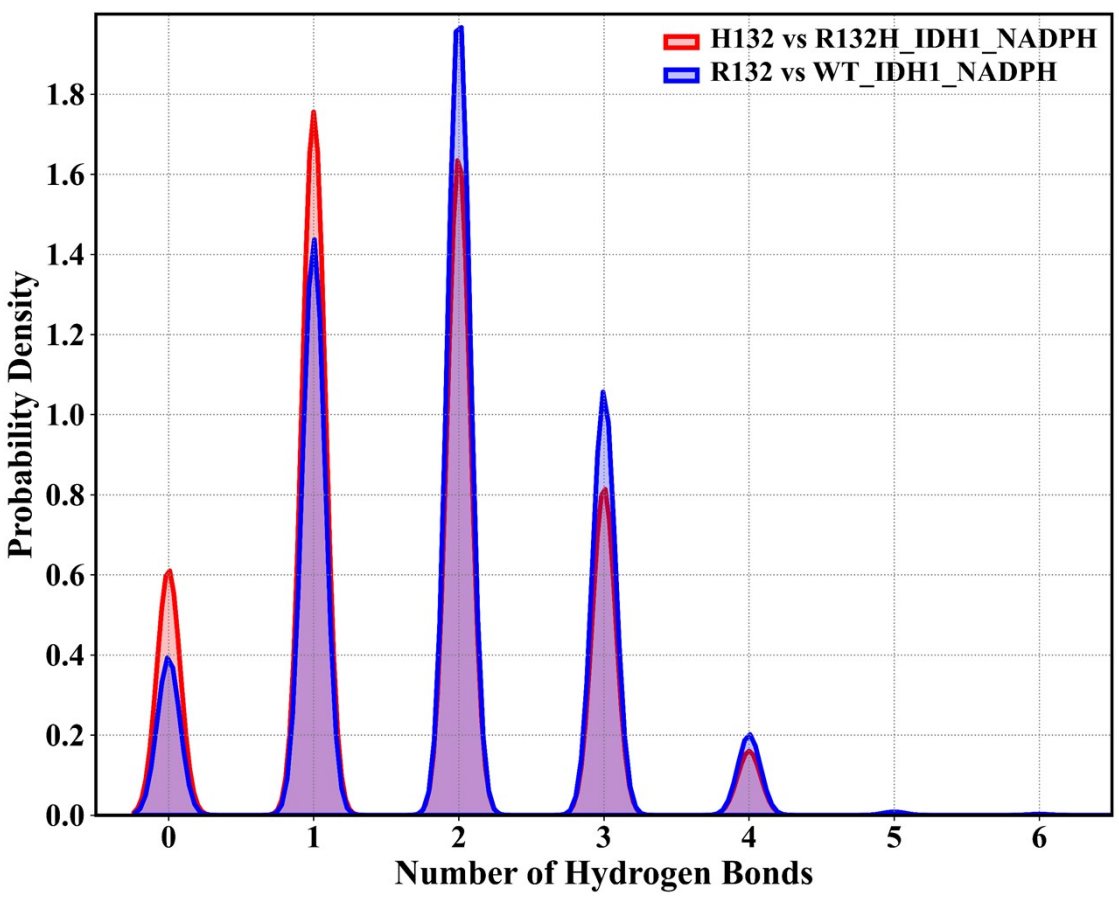


**Figure S17.** Distribution (kernel density estimation) of the tendency of mutant site to form the number of hydrogen bonds within its proximity for **(A)** apo form R132H_IDH1 and

WT_IDH1, **(B)** R132H_IDH1_ICT and WT_IDH1_ICT, and **(C)** R132H_IDH1_NADPH and WT_IDH1_NADPH.

**Table S10. Occupancy of hydrogen bonds between the R132 and other residues in the WT_IDH1.**

| WT_IDH1_No_Ligand | | |
|---|---|---|
| Donor | Acceptor | Occupancy |
| R132-Side | D275-Side | 84.33% |
| R132-Main | V107-Main | 10.11% |
| T106-Side | R132-Main | 1.98% |
| R132-Main | C269-Main | 1.29% |
| R132-Side | H133-Main | 5.43% |

**Table S11. Occupancy of hydrogen bonds between the H132 and other residues in the R132_IDH1.**

| R132H_IDH1_No_Ligand | | |
|---|---|---|
| Donor | Acceptor | Occupancy |
| H132-Main | V107-Main | 45.63% |
| H132-Main | C269-Main | 8.48% |
| N271-Main | H132-Side | 4.88% |
| H132-Side | D275-Side | 5.31% |
| H132-Side | N271-Main | 8.16% |
| V107-Main | H132-Main | 35.40% |
| V107-Side | H132-Main | 1.01% |

**Table S12. Occupancy of hydrogen bonds between the R132 and other residues in the WT_IDH1_ICT_NADPH complex.**

| WT_IDH1_ICT_NADPH | | |
|---|---|---|
| Donor | Acceptor | Occupancy |
| R132-Side | D275-Side | 50.99% |
| R132-Main | V107-Main | 12.20% |
| R132-Side | N271-Side | 7.66% |
| R132-Main | C269-Main | 1.68% |
| T106-Side | R132-Main | 23.07% |
| R132-Side | H133-Main | 5.47% |
| R132-Side | N271-Main | 4.48% |
| V107-Main | R132-Main | 1.69% |

**Table S13. Occupancy of hydrogen bonds between the H132 and other residues in the R132H_IDH1_ICT_NADPH complex.**

| R132H_IDH1_ICT_NADPH | | |
|---|---|---|
| Donor | Acceptor | Occupancy |
| H132-Main | V107-Main | 55.46% |
| T106-Side | H132-Main | 1.36% |
| H132-Side | D275-Side | 3.49% |
| R109-Side | H132-Side | 11.43% |
| H132-Side | N271-Main | 17.07% |
| G274-Main | H132-Side | 1.74% |

**Table S14. Occupancy of hydrogen bonds between the R132 and other residues in the WT_IDH1_ICT complex.**

| WT_IDH1_ICT | | |
|---|---|---|
| Donor | Acceptor | Occupancy |
| R132-Main | V107-Main | 13.11% |
| R132-Side | D275-Side | 81.00% |
| R132-Side | D79-Side | 9.32% |
| R132-Side | N271-Main | 1.17% |
| V107-Main | R132-Main | 1.29% |
| R132-Side | H133-Main | 5.17% |

**Table S15. Occupancy of hydrogen bonds between the H132 and other residues in the R132H_IDH1_ICT complex.**

| R132H_IDH1_ICT | | |
|---|---|---|
| Donor | Acceptor | Occupancy |
| T106-Side | H132-Main | 2.53% |
| H132-Main | V107-Main | 25.24% |
| H132-Side | S278-Side | 1.54% |
| H132-Side | D275-Side | 4.13% |
| N271-Side | H132-Side | 1.78% |
| R109-Side | H132-Side | 2.87% |

**Table S16. Occupancy of hydrogen bonds between the R132 and other residues in the WT_IDH1_NADPH complex.**

| WT_IDH1_NADPH | | |
|---|---|---|
| Donor | Acceptor | Occupancy |
| R132-Side | D275-Side | 13.50% |
| D275-Main | R132-Side | 1.64% |
| T106-Side | R132-Main | 4.61% |
| R132-Main | V107-Main | 27.10% |
| R132-Main | C269-Main | 2.15% |
| V107-Main | R132-Main | 7.02% |
| R132-Side | V107-Main | 2.58% |
| R132-Side | S278-Side | 3.59% |

**Table S17. Occupancy of hydrogen bonds between the H132 and other residues in the R132H_IDH1_NADPH complex.**

| R132H_IDH1_NADPH | | |
|---|---|---|
| Donor | Acceptor | Occupancy |
| H132-Main | V107-Main | 28.04% |
| T106-Side | H132-Main | 3.08% |
| H132-Side | S278-Side | 1.32% |
| H132-Main | C269-Main | 3.65% |
| N271-Side | H132-Side | 10.50% |
| R109-Side | H132-Side | 1.15% |
| H132-Side | R109-Side | 1.11% |
| V107-Main | H132-Main | 12.49% |
| H132-Side | D275-Side | 4.47% |
| H132-Side | N271-Main | 1.44% |

**Table S18. Pocket Parameters**

| Species | | Total SASA ($nm^2$) | Polar SASA ($nm^2$) | Apolar SASA ($nm^2$) | Volume ($Å^3$) |
|---|---|---|---|---|---|
| **Snapshot 1** | Pocket 1 | 517.08 | 297.29 | 219.79 | 1817.42 |
| | Pocket 2 | 270.03 | 114.35 | 155.78 | 887.98 |
| **Snapshot 2** | Pocket 1 | 474.63 | 288.66 | 185.97 | 1688.53 |
| | Pocket 2 | 273.58 | 138.01 | 135.57 | 1068.86 |
| **Snapshot 3** | Pocket 1 | 409.09 | 246.06 | 163.03 | 1308.27 |
| | Pocket 2 | 311.99 | 139.30 | 172.69 | 1138.22 |
| **Snapshot 4** | Pocket 1 | 334.57 | 201.73 | 132.84 | 869.55 |
| | Pocket 2 | 327.60 | 186.07 | 141.53 | 1192.10 |

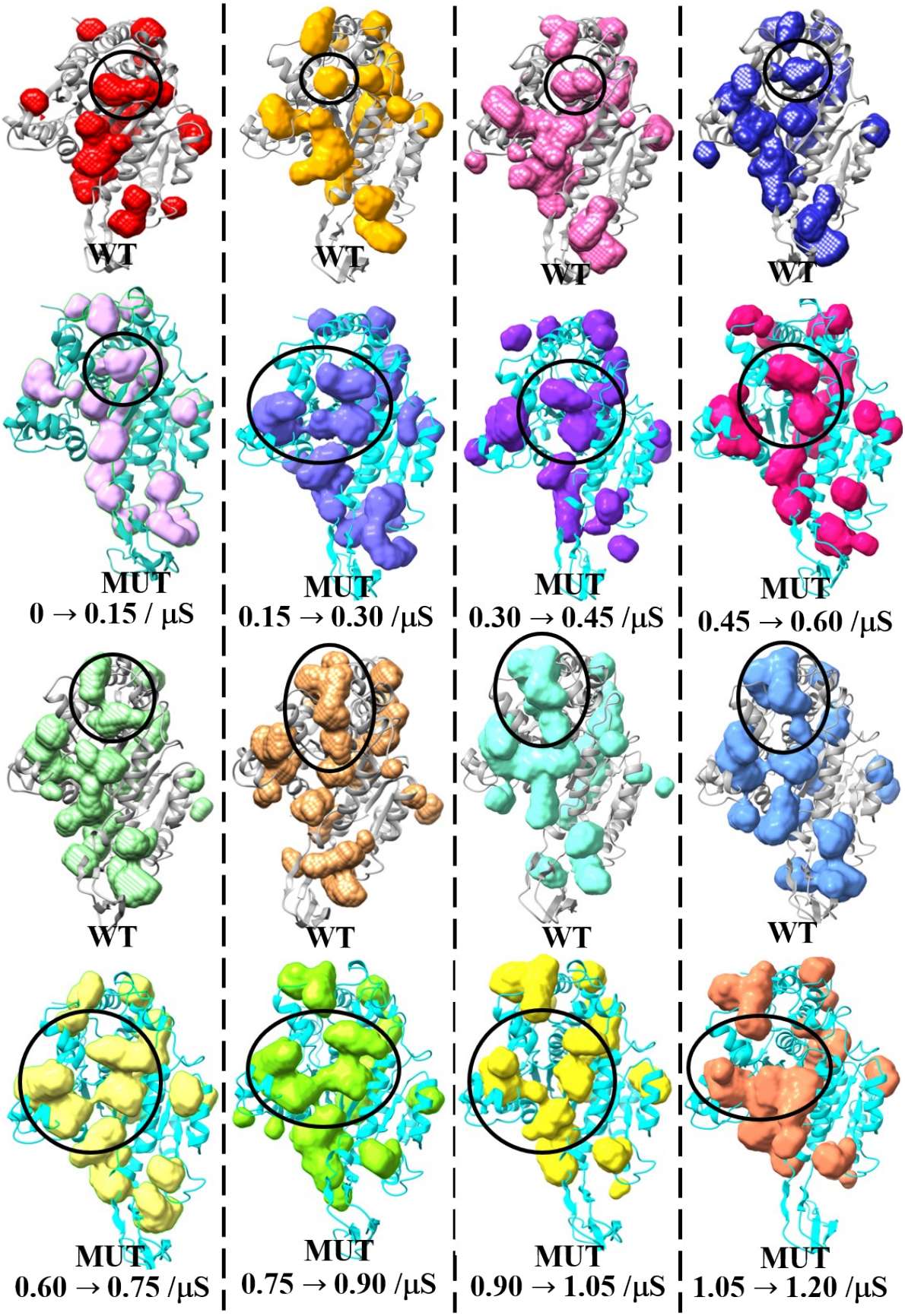
WT
WT
WT
WT
MUT
0 → 0.15 / μS
MUT
0.15 → 0.30 /μS
MUT
0.30 → 0.45 /μS
MUT
0.45 → 0.60 /μS
WT
WT
WT
WT
MUT
0.60 → 0.75 /μS
MUT
0.75 → 0.90 /μS
MUT
0.90 → 1.05 /μS
MUT
1.05 → 1.20 /μS

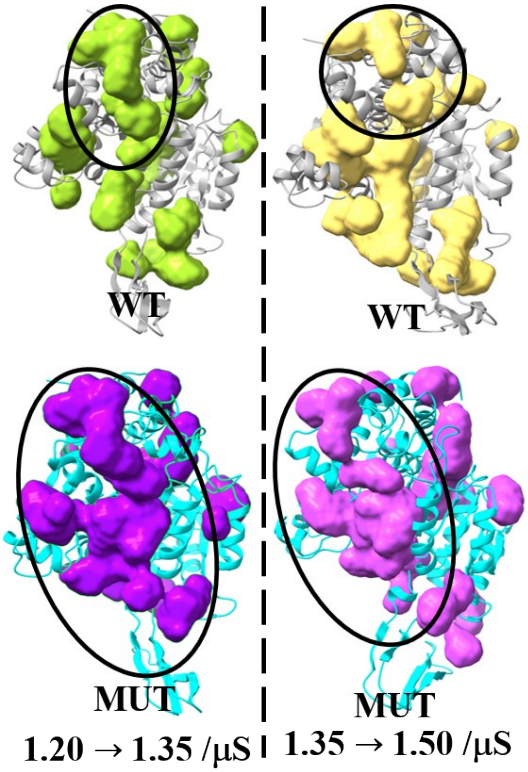


**Figure S18.** Representation of dynamically formed pockets in terms of pocket frequency (persistency) for R132H_IDH1 and WT_IDH1. For R132H_IDH1, it is evident from the figure that the pocket emerges (indicated by a circle) at 0.15 μs, keeps increasing till 0.60 μs, and then becomes stable till 1.05 μs. Further, at 1.05-1.20 μs, the pocket almost disappears, and it reappears in the segment 1.20-1.50 μs with an immensely large volume. Large volume is a consequence of the merging of various voids present within the proximity of the new and canonical binding site. Merging of voids is further a consequence of eminent disorderness in the R132H_IDH1, which dominates in the last ~400 ns of the simulation. While for WT_IDH1, the pocket (indicated by a circle) is stable across all the segments along the small variation in volume, which can be attributed to the normal breathing of WT_IDH1.